

**DEVELOPMENT OF VARIABLE CHANNEL- SPACED L-BAND MULTI-
WAVELENGTH BRILLOUIN ERBIUM FIBER LASER**

JELEEL ALAO OLADAPO

SPS/12/MEE/00002

**A THESIS SUBMITTED TO THE POSTGRADUATE SCHOOL OF
BAYERO UNIVERSITY, KANO, IN PARTIAL FULFILLMENT OF
THE REQUIREMENTS FOR THE AWARD OF MASTERS OF
ENGINEERING(COMMUNICATIONS) DEGREE.**

NOVEMBER, 2015.

DECLARATION

I hereby declare that I carried out the work reported in this dissertation in the Department of Electrical Engineering, BayeroUniversity, Kano under the supervision of **Dr. M. Ajiya**. I also solemnly declare that to the best of my knowledge, no part of this dissertation has been submitted here or elsewhere in a previous application for award of a degree. All sources of knowledge used have been duly acknowledged.

.....
OLADAPO, JELEEL ALAO

SPS/12/MEE/00002

CERTIFICATION

This is to certify that the thesis titled “Development of Variable Channel-Spaced L-band multi-wavelength Brillouin Erbium Fiber Laser” by Oladapo, JeleelAlao (SPS/12/MEE/0002), meets the requirements and regulations governing the award of the Master of Engineering (Communication) degree of Bayero University, Kano and is approved for its contribution to knowledge and literary presentation

Supervisor
Dr. M. Ajiya Date

P.G. Coordinator
Dr. N. Magaji Date

Head of Department
Dr. S.B.Ibrahim Date

External Examiner
Date

APPROVAL

This dissertation has been examined and approved for the award of master in (Communication Engineering).

Thesis Supervisor

Dr. M. Ajiya

Internal Examiner

Dr. D. S. Shu'aibu

External Examiner

Head of Department

Dr. S. B. Ibrahim

ACKNOWLEDGEMENT

My deepest gratitude goes to my supervisor, Associate Professor Mohammed Ajiya for his guidance and support. I really benefited from working with him both professionally and intellectually. More importantly, I have benefited tremendously from his broad range of experience, technical insights, vision, inspiration and enthusiasm for research. In fact, I appreciate his care, patience and dedication in constructively criticizing my research work and thesis as well. Also, I would like to thank all lecturers and member staffs of the department of Electrical engineering, Bayero University Kano for their strong academic support and encouragement that lead to the completion of this thesis. Without them it would have been a toughest time. I thank you all.

I would as well like to thank my colleagues, AbubakarBuba Bello, KaluChinedu Joseph, Hassan Taiwo, Desmond Ezegwu, FaleyeAdeola Michael, Moshood Ismail and YakoobMuktar for their friendship, support, and encouragement. Finally, I thank all the members of my family most especially my wife for her support, encouragement and constant love which has been my source of patience, inspiration, motivation, courage and strength.

DEDICATION

This project is dedicated to my parents, late Mr. and Mrs. Oladapo, who gave me good background from the onset. May their soul rest in perfect peace (Amen).

TABLE OF CONTENTS

Declaration	ii
Certification	iii
Approval	iv
Acknowledgment	v
Dedication	vi
Tables Of Contents	vii
List Of Tables	x
List Of Figures	xi
List Of Abbreviation	xv
List Of Appendices	xvii
Abstract	xviii
 CHAPTER ONE: INTRODUCTION	
1.1 Background	1
1.2 Motivation	2
1.3 Problem Statement	3
1.4 Research Aim and Objectives	3
1.5 Scope of the Work	4
1.6 Limitation of the work	4
1.7 Organization of the Thesis	4
 CHAPTER TWO: LITERATURE REVIEW	
2.1 Introduction	6
2.2 Scattering of Light in Optical Fiber	7
2.2.1 Types of Scattering	7
2.2.2 Basic Concept of SBS	9
2.2.3 Brillouin Parameter	10
2.2.4 SBS Applications	11
2.3 Laser	13
2.3.1 Principle of Laser	13
2.3.2 Types of Laser	15
2.3.3 Linear Cavity	16
2.3.4 Ring Cavity	17
2.4 Fiber Based Laser	18
2.4.1 Multi-wavelength Fiber laser	18
2.4.1.1 Erbium Doped Fiber Laser	18
2.4.1.2 Brillouin Fiber Laser	19
2.4.1.3 Brillouin Raman Fiber Laser	20
2.4.1.4 Brillouin/Erbium Fiber Laser	21
2.5 Previous Works on MWBEFL	23

CHAPTER THREE: METHODOLOGY

3.1	Introduction	31
3.2	Principle of Operation of Simulation Set Up	31
3.3	Optisystem Library Component used in MWBEFL Design	32
3.3.1	Continuous wave Laser	33
3.3.2	Brillouin Pump	33
3.3.3	Optical Circulator	33
3.3.4	Optical Isolator	34
3.3.5	Optical Amplifier	35
3.3.6	Delay Interferometer	35
3.4	Brillouin Fiber Laser Parameters	36
3.4.1	Design Parameters	37
3.4.1.1	Brillouin Pump Power	37
3.4.1.2	Brillouin Pump Wavelength	37
3.4.1.3	EDFA Gain	38
3.4.1.4	Time Delay	39
3.4.2	Performance Parameters	39
3.4.2.1	The Output Channel Peak Power	39
3.4.2.2	Threshold Power	40
3.4.2.3	Number of Channels generated	40
3.4.2.4	Tuning Range	41
3.4.2.5	Optical Signal to Noise Ratio (OSNR)	41
3.5	Conclusion	42

CHAPTER FOUR: RESULT AND DISCUSSIONS

4.1	Introduction	43
4.2	Effect of EDFA Gain	43
4.2.1	The Effect of EDFA Gain on Threshold	44
4.2.2	Effect of EDFA Gain on Channel (Stokes and anti-Stokes Peak Power)	48
4.2.3	Effect of EDFA Gain on Number of Channels (Stokes and anti-Stokes Signal)	49
4.3	Effect of Brillouin Pump Power	51
4.3.1	Effect of Brillouin Pump power on Stokes and Anti-Stokes Peak Power	52
4.3.2	Effect of Brillouin Pump Power on the Number of Channel (Stokes and Anti-Stokes Signal)	54
4.4	Effect of Brillouin Pump Wavelength	55
4.4.1	Effect of Brillouin Wavelength on Number of Output Channels and Total output Channel	55
4.5	Effect of Time Delay	57
4.5.1	Effect of Interferometer Time Delay On Channel Spacing	57

4.5.2 Effect of Interferometer Time Delay on Number of Output Channels Generated	58
4.6 Optical Signal to Noise Ratio (OSNR) Analysis	59
4.6.1 Effect of Brillouin Pump Power on OSNR	60
4.6.2 Effect of EDFA on OSNR	61
4.7 Major Contributions	63
CHAPTER FIVE: SUMMARY, CONCLUSION AND RECOMMENDATION	
5.1 Summary	65
5.2 Conclusion	66
5.3 Recommendation for Future Works	67
REFERENCES	69
APPENDIX A	73
APPENDIX B	78

LIST OF TABLES

2.1	Summary of Previous work reviewed	30
3.1	Details specification of three port circulator used	34
3.2	Details specification of comb filter delay interferometer used	36

LIST OF FIGURES

2.1	Block diagram of research design	6
2.2	Schematic Diagram of the observed scattered light intensity	7
2.3	Light Scattering Without Change in Frequency	8
2.4	Basic Stimulated Brillouin Scattering Mechanism	10
2.5	The principle structure of a laser cavity	13
2.6	Energy level diagram in a three level laser	142.7
	Schematic Diagram of All-Fiber Fabry-Perot Cavity	17
2.8	Schematic Diagram of All-Fiber Ring Cavity	17
2.9	Schematics Diagram of the BEFL configuration	21
2.10	Schematics Diagram of BEFL operations	22
2.11	Experimental setup of the internal cascade technique used to generate multiple wavelengths.	24
2.12	Spectrum of the BEFL for various 980 nm pump power	24
2.13	Experimental setup of a multi-wavelength BEFL utilizing a Fabry–Perot resonator in the L-band region	25
2.14	Optical spectrum of 24 cascaded Stokes with BP power set at 0.18mW	25
2.15	Experimental setup of a linear cavity multi-wavelength L-band Brillouin-Erbium comb fiber laser	26
2.16	Output spectrum from both BEFL configurations at pump power of 73mW, BP power and wavelength are set at 1.1mW and 1603.1 nm respectively.	26
2.17	Schematic diagram of a linear cavity MWBEFL with double-pass BP pre-amplified technique	27

2.18	Output spectrum at different BP and 1480 nm pump powers at 0.035mW and 40mW	27
2.19	Experimental setup of multi-wavelength BEFL utilizing nonlinear AFLMF.	28
2.20	24-Stokes Channel Output spectra of MWBEFL utilizing nonlinear AFLMF	28
2.21	Configuration of the multi-wavelength BEFL with double spacing	29
2.22	Output spectrum of the MWBEFL with BP power of 3dBm and 50mW pump power	29
3.1	BFL Simulation Set Up in Optisystem	32
3.2	Schematic Diagram of Three Port Circulator	34
4.1	Output spectrum of no lasing condition in the cavity at EDFA Gain of 5dBm	44
4.2	Output spectrum of lasing condition in the cavity at EDFA gain of 10dB	45
4.3	Power characteristics of the BEFL as a function of the launched EDFA gain	45
4.4	Lasing threshold of the delay Interferometer assisted MBEFL laser System	46
4.5	The Stokes and anti-Stokes (total output channel) signals lasing Threshold as a measure of EDFA gain	47
4.6	Stokes peak power plotted against Stokes signal order at different EDFA gain	48
4.7	Anti-Stokes peak power plotted against Stokes signal order at different EDFA gain	49

4.8	Number of Output channels (Stokes and anti-Stokes signals)	50
	Generated against EDFA gain	
4.9	Wavelength spectrum of EDFA gain above optimum	50
4.10	Thirty one output channels, 0.17nm (20GHz) spacing of Brillouin	51
	Fiber laser comb	
4.11	Wavelength spectrum of Brillouin power above optimum	52
4.12	Stokes peak power plotted against Stokes signal order at different	53
	BP power	
4.13	Anti-Stokes peak power plotted against Stokes signal order at	53
	Different BP power	
4.14	Number of Output channels (Stokes and anti-Stokes signals)	54
	Generated against BP power	
4.15	Number of output channels generated against BP wavelength	55
4.16	Total output power against BP wavelength	56
4.17	Wavelength channel spacing against time delay of the delay	57
	Interferometer	
4.18	Output Channels generated against wavelength channel spacing	58
4.19	Output Channels (Stokes and anti-Stokes signal) OSNR corresponding	60
	to EDFA Gain and Brillouin power of 10dB and 6dBm	

4.20	Stokes signal OSNR at different Brillouin pump power	61
4.21	Anti-Stokes signal OSNR at different Brillouin pump power	61
4.22	Stokes signal OSNR at different EDFA gain	62
4.23	Anti-Stokes signal OSNR at different EDFA gain	63

LIST OF ABBREVIATIONS

ASE	-	Amplified Spontaneous Emission
AWG	-	Waveguide Grating
BEFL	-	Brillouin Erbium Fiber Laser
BER	-	Bit Error Rate
BFL	-	Brillouin Fiber Laser
BP	-	Brillouin Pump
BRFL	-	Brillouin Raman Laser
BSL	-	Brillouin Stokes Line
C-Band	-	Conventional Band
COIL	-	chemical oxygen iodine laser
CW	-	Continuous Wave
CCW	-	Counter Clockwise
CW	-	Clockwise
DI	-	Delay Interferometer
DWDM	-	Dense Wavelength Division Multiplexing
EDF	-	Erbium Doped Fiber
EDFA	-	Erbium Doped Fiber Amplifier
EDFL	-	Erbium Doped Fiber Laser
EM	-	Electromagnetic
ESA	-	Excited Absorption
FP	-	Fabry-Perot

FWM	-	Four Wave Mixing
L-Band	-	Long wavelength Band
LD	-	Laser Diode
LED	-	Laser Emitting Diode
MWBEFL	-	Multi-wavelength Brillouin Erbium Fiber Laser
MWBFL	-	Multi-wavelength Brillouin Fiber Laser
MWBRFL	-	Multi-wavelength Brillouin Raman Fiber Laser
OSA	-	Optical Spectrum Analyzer
OSNR	-	Optical Signal to Noise Ratio
SBS	-	Stimulated Brillouin Scattering
SMF	-	Single Mode Fiber
TLS	-	Tunable Laser Source
VCSEL	-	Vertical cavity surface-emitting laser
WDM	-	Wavelength Division Multiplexing

LIST OF APPENDICES

A	Output spectra of the Brillouin wavelength tuning	74
B	Output spectra of the variation of time delay for channel spacing analysis	79

ABSTRACT

The broadband applications in optical communication system demands for large number of channel and bandwidth in order to increase the transmission capacity, Meanwhile multi-wavelength fiber laser operating in the long-wavelength band (L-band) region is needed as laser source due to its applications especially in dense wavelength-division-multiplexed (DWDM). Majority of the multi-wavelength fiber lasers developed so far are faced with the problems of inability to produce wide spacing between the adjacent channels, large number of channels with wide tuning range. The objective of this research is to develop a fiber laser that will tackle these shortcomings, therefore a multi-wavelength Brillouin erbium fiber laser (MWBEFL) with adjustable spacing between adjacent channels and operating in L-band region has been developed with optical components in optical simulation software called optisystem. This developed fiber laser is simulated in this optisystem software environment. The effect of input parameters (EDFA gain, time delay (propagation delay), Brillouin pump power (BPP) and wavelength) on performance parameters (threshold power, channel peak power, tuning range, channel spacing, number of channel produced and optical signal to noise ratio (OSNR)) were properly analyzed. The laser exhibits threshold power in term of EDFA gain of 10dB (10mW) with time delay at 0.05ns and very low BPP of -65dBm (0.0003162 μ W) for first Stokes channel generation and about 31-output channels with double Brillouin shift of about 0.17nm were produced with EDFA gain of 30dB to 80dB. With time delay at 0.1ns about 64 output channels are produced with channel spacing of 0.08nm and that the output channel decreases with increase in channel spacing as the value of the time delay is decreasing. With optimum BPP at 6dB, maximum of 31-output channels of 16-Stokes and 15-anti-Stokes were obtained with 37nm bandwidth within the tuning range in L-band range of 1588nm-1625nm and the peak powers of first and sixteenth Stokes are -23.26dBm and -52.00dBm, with OSNR of 30.03dBm and 7.21dBm respectively, while the first and fifteenth anti-Stokes peak powers are -27.60dBm and -44.66dBm with OSNR of 25.69dBm and 6.63dBm respectively which indicates that better OSNR is obtained for the channel with high peak power.

CHAPTER ONE

INTRODUCTION

1.1 Background

Laser source is one of the most important devices in optical communication system. It serves purpose of carrier light in fiber and information to be transmitted is modulated on the carrier light by optical modulator. Due to the security, reliability and huge bandwidth or capacity, light is widely been used to transmit information over large distance. The telecommunication industry has tremendously progressed for capacity over last few years due to the rapid growing usage of the broadband applications, specifically in internet and data transfer. Other broadband applications include, voice, high resolution images, videophones, videoconferencing, video-on-demand and multimedia applications. The demand for this high capacity can be met by dense wavelength division multiplexing (DWDM). DWDM is multiplexing technique in a light wave system that consists of a large number of spaced wavelength sources.

Optical amplifier also plays important role as it compensates for loss in transmission optical fiber and optical devices (such as add/drop multiplexers and optical switches) that make up a network and enable greater network scale and transmission distances. Therefore the combined performance of amplifier and DWDM claim to be more prudent in the cost of upgrading and installation.

On the other hand, sophisticated laser modules which comprise of highly stabilized laser diodes are used as optical source in the DWDM systems. Also sophisticated monitoring unit of laser output is required to prevent cross talk. This makes the optical communication system more complex.

Besides the laser diodes, multi-wavelength can also be generated using fiber laser. Multi-wavelength fiber laser attracts considerable interest due to its various applications, especially for the use in the DWDM (Bellemare et al., 2000), microwave photonics, optical component testing, spectroscopy application (Micheli et al., 2010), optical signal processing and sensor application such as, gas sensing [Mishra et al., 2014], vibration sensor (Taiwo et al., 2014) and laser gyroscope (Zarinetchi et al., 1991) and soon. The fiber laser can be constructed using any type of fiber as a nonlinear gain medium. The nonlinearity in an optical fiber such as, stimulated Raman scattering (SRS) (Zhao and Jackson, 2005) and stimulated Brillouin scattering (SBS) (Smith et al., 1991) are commonly used to generate multiple channels with ultra-narrow wavelength spacing. This multi-wavelength source provides a cheap and efficient alternative to the deployment of multiple laser diodes at different wavelengths. It is also compact, consumes less energy, compatible with other optical fiber components and generates less heat as compared to multiple diode system.

1.2 Motivation

The availability of fiber lasers at all the optical communications transmission windows and its compatibility with existing communications systems place fiber lasers in a strategic position for applications in optical communications. Based on this fact, bandwidth extension requirement by broadband application can be satisfied. Therefore, MWBEFL considered in this research will be operating in L-band to enlarge the transmission capacity.

The fiber laser with proper configuration arrangement produces higher number of channels which makes it suitable to be used in DWDM application. The higher number of output

channels which can be tuned at a wider range is possible in the MWBEFL implemented in this research.

More so, fiber laser with adjustable channel spacing can be useful for many applications and also expanding the spacing between adjacent channels more than narrow 10GHz is a very great achievement of the fiber laser. In view of this, comb filter termed delay interferometer is included in the MWBEFL considered in this research to have control over the spacing, so that MWBEFL can be tuned at any desired channel spacing to suit any application.

1.3 Problem statement

The broadband applications in optical communication system demand for higher number of channel and bandwidth in order to increase the transmission capacity, therefore amplification bandwidth of the rare-earth doped optical fiber amplifiers in fiber laser must be expanded beyond the C-band, thus extending the bandwidth beyond C-band is desired and suitability of fiber laser in DWDM application requires larger number of channels, so that the need for transmission capacity can be satisfied.

Most of the fiber lasers are facing difficulty in channel de-multiplexing, due to the narrow spacing in order of 10GHz between adjacent channels. There is need for the fiber based laser with adjustable channel spacing between adjacent channels, so that the spacing can be tuned to suit different applications.

1.4 Research Aim and Objectives

The aim of this research is to develop a variable channel-spaced multi-wavelength Brillouin erbium fiber laser that operates in the L-band of the low loss optical communication window. The objectives of this research are:

- (1) Development and simulation of a MWBEFL using the optisystem library components..
- (2) Determination of optimum design of the MWBEFL to obtain variable number of channels and spacing at a higher signal peak power that can be tuned at a wider range.

1.5 Scope of the Work

The scope of this study is limited to simulation carried out in optisystem, optical system simulation software developed by optiwave system Inc.

1.6 Limitation of the Work

This research is limited in some areas, for instance the study is limited to analyzing the performance parameters such as threshold, channel spacing, peak power, tuning range and OSNR only. Stability study is not included. Also, only transmitted signal was considered during the analysis and the study silent on reflected signal. The flatness in peak power and effect of single mode fiber (SMF) length on MWBEFL performance were not covered.

1.7 Organization of the Thesis:

The first chapter presents the introductory background of the multi-wavelength laser source, also the problem statement, motivation, scope, aim and objectives and limitation of the project were clearly stated in this chapter. Chapter two presents theory of scattering including the types of scattering with details in Stimulated Brillouin scattering (SBS). Also, the theory of laser including the types and principle were discussed but detailing in multi-wavelength fiber laser (MWFL) with focus on multi-wavelength Brillouin erbium fiber laser (MWBEFL). The previous works on MWBEFL in L-band region is also reviewed in this chapter. Chapter three tagged the

methodology of the thesis. The research design as well as operating principle of the multi-wavelength fiber laser considered in this thesis was properly discussed in this chapter. The input and output parameters used in studying the multi-wavelength laser in this study are also discussed in details in this chapters. Chapter four presents all the simulation results from the optisystem software. The performance analysis through performance parameter is done by presentation through Microsoft excel plotted graphs and spectrum obtained from the result of the simulation for the better understanding of the analysis. The summary result of the analysis is also contained in this chapter. Chapter five concludes the findings of this simulation research and provides therecommendation for future studies for the further development of this multi-wavelength fiber laser system.

CHAPTER TWO

LITERATURE REVIEW

2.1 Introduction

This chapter introduces the concept of light scattering in optical fiber and its various types. The fundamental principle of laser and various types of lasers were briefly discussed but detailing in fiber lasers especially MWBEFL that is the core of this research. Previous works of MWBEFL are also presented. The summary of discussion in this chapter is shown in block diagram in figure 2.1

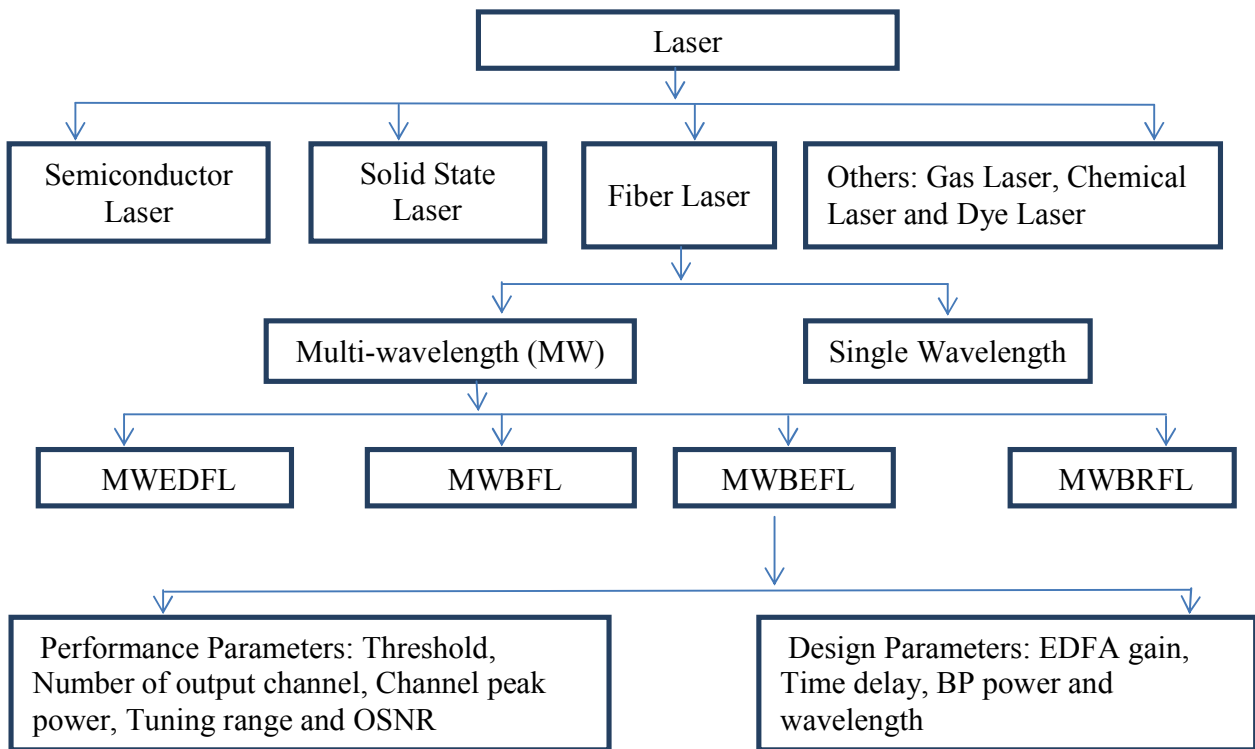


Figure 2.1: Block diagram of research design

2.2 Scattering of Light in Optical Fiber

When an electro-magnetic (EM) wave (Jackson, 1962), or light, is launched into a material such as an optical fiber, the incident EM wave interacts with the molecules of the material, resulting in a scattering phenomenon. The result is a scattering spectrum. Depending on the intensity of the incident light, we may get either spontaneous scattering for low intensities of incident light, or stimulated scattering for high intensities of incident light. Figure 2.2 shows a typical spectrum for scattering from solid state matter. In inelastic scattering, the light having a lower frequency than the incident light is called the Stokes branch, while the light having a higher frequency than the incident light is called the anti-Stokes branch.

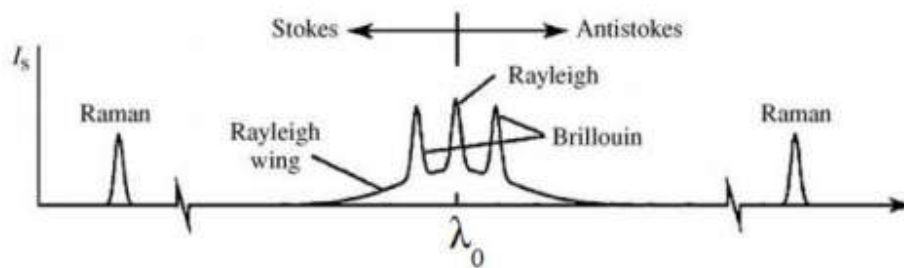


Figure 2.2: Schematic of the observed scattered light intensity (Boyd, 1992).

2.2.1 Types of Scattering

Two basic types of scattering exist. This includes linear and nonlinear scattering. The linear scattering consists of Mie and Raleigh scattering while nonlinear scattering includes Brillouin and Raman scattering. These scattering phenomena are briefly discussed as follows:

(1) Rayleigh scattering: It is related to the irregularities due to the material structure. Air and glass are well known examples where the small refractive index fluctuations induced by their amorphous nature can scatter light in all directions (Palais, 1998). This is done without changing

the frequency of the scattered light; because the irregularities are frozen in the material structure as shown in Figure 2.3

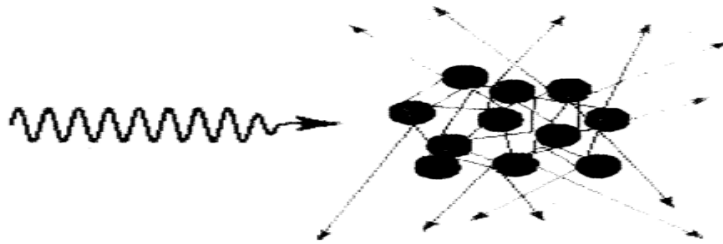


Figure 2.3: Light Scattering Without Change in Frequency (Rayleigh Effect).

(2) **Brillouin Scattering:** Brillouin scattering arises from the interaction of light with acoustic waves that are always present in any material. Acoustic waves modulate the refractive index (photo-elastic effect); thus a low power laser traversing the medium is scattered with a different frequency. In the backward direction the frequency shift is larger and of the order of 10 GHz in silica fiber. Brillouin scattering can either be Spontaneous or stimulated in case of high intense light travelling in a medium, such as an optical fiber.

(3) Raman scattering: is another form of inelastic light scattering, but instead of scattering from acoustic phonons, as in Brillouin scattering, the light interacts with optical phonons, which are predominantly intra-molecular vibrations and rotations with energies larger than acoustic phonons.

(4) Mie scattering: is a broad class of scattering of light by spherical particles of any diameter. The scattering intensity is generally not strongly dependent on the wavelength, but is sensitive to the particle size. Mie scattering coincides with Rayleigh scattering in the special case where the

diameter of the particles is much smaller than the wavelength of the light; in this limit, however, the shape of the particles no longer matters. Mie scattering intensity for large particles is proportional to the square of the particle diameter.

2.2.2 Basic Concept of SBS

The SBS is a nonlinear process that can occur in optical fibers at large intensity. Quantum mechanically the Brillouin shift originates from the photon to phonon interaction. The basic mechanism of SBS phenomenon is illustrated in Figure 2.4. The pump wave creates acoustic wave in transmission medium through a process called electrostriction. The interaction between pump wave and acoustic wave creates the generation of back propagating optical wave which is called Stokes wave. When acoustic waves travel through the solid, transparent glass material, they induce spatially periodic local compressions and expansions which in turn cause local increases and decreases in the refractive index. This phenomenon is known as photo-elastic effect. The magnitude of the photo-elastic effect increases with increasing input optical power. When the input power reaches a SBS threshold level, the refractive index of the fiber has been acoustically altered to a degree such that a significant portion of the optical signal is back-scattered. So, one can say that the acoustic wave alters the optical properties of the fiber, including the refractive index. This fluctuation of refractive index scatters the incident wave and creates Stoke wave which propagates in the opposite direction.

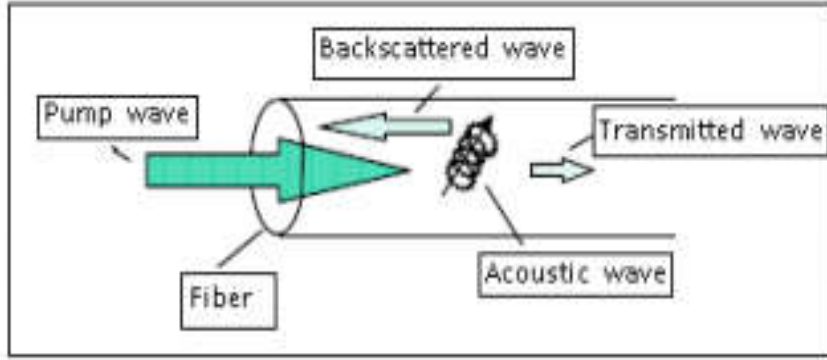


Figure 2.4: Basic Stimulated Brillouin Scattering Mechanism

2.2.3 Brillouin Parameter

The Brillouin parameters include Brillouin shift, Brillouin threshold and Brillouin gain. These parameters can be explained by considering the SBS effect in optical fiber. In a single mode optical fiber, only relevant directions are described as forward and backward. For this reason, SBS occurs only in the backward direction with the Brillouin shift ($\Delta\nu_s$) given as shown in equation 2.1

$$\Delta\nu_s = V_B = \omega_A / 2\pi = \frac{2nV_A}{\lambda_p} \quad (2.1)$$

Where n is the fiber refractive index of the medium, V_A is the speed of the sound in the medium and λ_p is the pump wavelength. The Stokes frequency shift can also be expressed as Stokes wavelength shift using,

$$\Delta\lambda_s = C\Delta\nu_s \quad (2.2)$$

Where constant $C = \lambda_p^2 / c$, c is the speed of light in vacuum. In the case of silica optical fiber if $V_A = 5.96 \text{ km/s}$ and $n = 1.45$, $\lambda_p = 1550 \text{ nm}$, the value appropriate Brillouin shift for silica fibers is, $V_B \approx 10 \text{ GHz}$. Substituting this value into equation (2.1) gives the Stokes wavelength shift, denoted as Brillouin shift, $\Delta\lambda_s \approx 0.08 \text{ nm}$ which is equivalent to 10 GHz frequency spacing.

SBS introduces the most stringent power limit, commonly referred to as the Brillouin threshold, for the amplification or even passive propagation of narrow-band optical signals, such as those used in telecommunications (Ruffin, 2004). The SBS threshold can be expressed as in equation 2.3.

$$P_{th} \cong 21bA_{eff} / g_B L_{eff} \quad (2.3)$$

Where, g_B is the peak value of the Brillouin gain which is expressed as shown in equation 2.4

$$g_B = g_0 = \frac{2\pi^7 p_{12}^2}{c\lambda_p^2 \rho_0 V_A \Delta\nu_B} \quad (2.4)$$

The numerical factor of 21 is only approximate as it depends on the exact value of Brillouin-gain line width. The value of polarization factor b lies between 1 and 2 depending on relative polarization of pump and Stokes waves (Stolen, 1979). Typically $A_{eff} \approx 50\mu m^2$, $L_{eff} \approx 20km$ and $g_B = 4 \times 10^{11} m/W$ for an optical communication system at 1550nm. With these values and taking $b=1$, $P_{th} \approx 1.3mW$. Because of such a low value of threshold level, the SBS process is a dominant nonlinear process in fibers. The threshold power becomes just double if polarization factor b is taken equal to 2. The threshold power (P_{th}) depends mainly on the Brillouin gain (g_B). The fiber inhomogeneousness affects g_B and hence P_{th} . The variation in dopant also affects SBS threshold power up to some extent.

2.2.4 SBS Applications

SBS has many possible applications in the areas of optics and optical communications such as narrow band amplification, lasing, sensing, phase conjugation and slow light generation (Ippen and Stolen, 1972). SBS in optical fiber has been used for reduction of optical carrier of microwave signal (Loayssa et al., 2000). When the power of a weakly intensity-modulated

carrier exceeds the Brillouin threshold, it is converted to the backward propagating Stokes wave and is, therefore, selectively depleted. In such application, a single-mode Stokes wave is found to be more suitable compared with multimode in preventing the addition of noise (Norcia et al., 2003). Furthermore, Brillouin scattering is an efficient nondestructive and noncontact measurement method to obtain the wave properties of thin layers at hypersonic frequencies. This technique was applied for the nondestructive measurement of anisotropy and refractive indices of thin and polycrystalline ZnO films by introducing the Voigt function to obtain the Brillouin shift frequencies. The obtained refractive indices were similar with those of Abbe refractometer or the single crystal (Matsukawa et al., 2006). In another case, with the development of the very high contrast multi-pass interferometer it is now possible to perform measurements on very small and imperfect crystals and even on opaque materials where the penetration depth of the light is as low as a few wavelengths (Sandercock, 1975).

The effect of gamma-radiation on the physical properties of Brillouin scattering in commercially available optical fibers has been investigated up to very high total gamma doses. The frequency shift due to the ionizing radiation is about 5 MHz for the worst case. Distributed sensors based on stimulated Brillouin scattering can thus be considered to be radiation tolerant up to total doses of about 100K Gy, provided that the signal-to-noise ratio is kept at acceptable value. Distributed fiber sensors based on Brillouin spectral analysis can be an efficient monitoring tool for nuclear facilities. Further work on different fibers with different dopant concentration types will indicate which fiber is more suitable for nuclear environments. In addition, the use of the radiation-induced Brillouin shift as a tool of analysis will certainly bring new perspectives in the understanding of the compaction mechanism in irradiated amorphous silica (Alasial et al., 2006).

The Brillouin scattering method was also employed in a measurement of spectroscopic properties of materials (Kasprowicz et al., 2007). The temperature variation changes the values of Brillouin shift. The SBS effect can also be used to generate narrow line-width fiber laser as reported in many literatures (Boyd, 2007) and also in this thesis. The Brillouin fiber laser (BFL) has many potential applications for WDM communications, fiber optic sensors and others.

2.3 Laser

LASER is an acronym for light amplification by stimulated emission of radiation. As indicated in its name, a laser produces intense high-powered beams of coherent light by stimulated emission (Siegman, 1986). For lasing operation there must be an active medium where an inverted population must be created, energy pumping, continuous or in pulses, to sustain the inversion of population and optical resonator, to confine the light produced in a few cavity modes of the radiation field as shown in figure 2.5. The first publication on lasers was credited to Schawlow and Townes in 1958.

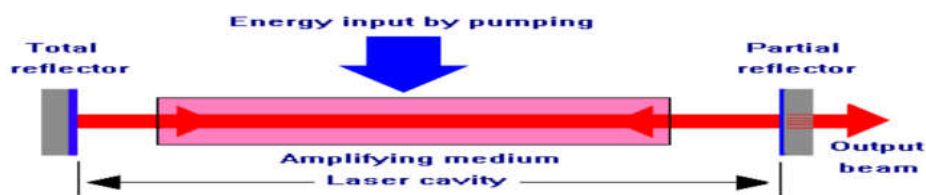


Figure 2.5: The principle structure of a laser cavity

2.3.1 Principle of Laser

The principle of a laser is based on four important processes such as absorption, spontaneous emission, stimulated emission within an amplifying medium and population inversion. When appropriate energy is supplied to the atom, electrons can jump from low-energy orbitals (E_1 : ground state) near the nucleus to high-energy orbitals further away (E_3), leading to

atomic excitation by the process of energy absorption. Some of the electrons in the high-energy orbit(E_2) spontaneously return to the ground state (E_1), releasing the difference in energy in the form of a photon, with a wavelength which depends exactly upon the difference in energy of the two states and has a random phase and direction. This process is called spontaneous emission. This emitted photon can collide with one of the mirrors in the resonating cavity and reflect back into the lasing medium causing further collision with some of the already excited atoms. If an excited atom is struck, it can be stimulated to decay back to the ground state, releasing two photons identical in direction, phase, polarization and energy (wavelength). This process is termed stimulated emission. The cascade effect of stimulated emission of photons occurs, resulting in further amplification (optical gain). For a laser to sustain functioning, the majority of the atoms must be maintained in the excited state, hence called “population inversion”. This is achieved by the continuous input from the energy pump (continuous wave laser) or by intermittent pumping resulting in a pulsed wave laser. The energy level diagram shown in Figure2.6 illustrates this process.

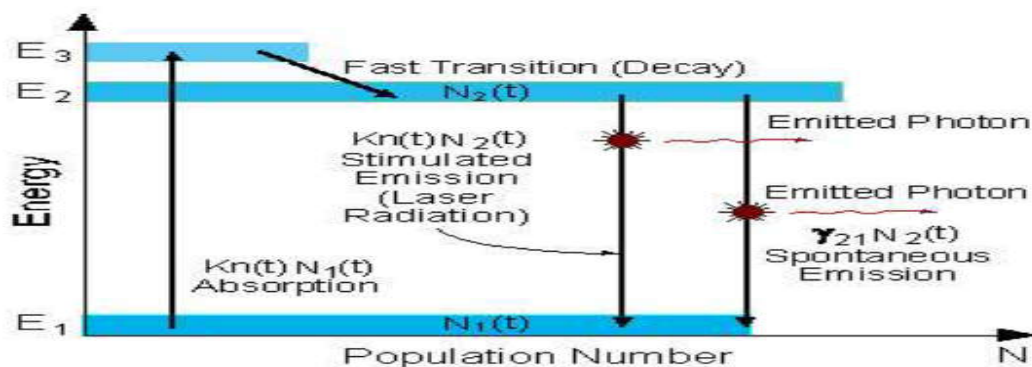


Figure 2.6: Energy level diagram in a three level laser

2.3.2 Types of Laser

Townes and Schawlow, 1958 extended the principle of the maser (microwave amplification by stimulated emission of radiation) to optical domain. In (Maiman, 1960) invented the first ruby laser. Since then, many lasers have been developed and built. Based on the active media laser can be categorized as follows:

(1) Solid-state lasers: the active medium is a solid at room temperature, e.g., crystal, glass or optical fiber. Generally, the medium will consist of a glass or crystalline host material to which is added a dopant such as neodymium, chromium, or erbium. Common dopants are rare earth elements. Common solid-state lasers are Nd: YAG, Ti: sapphire and Yb: glass lasers.

(2) Semiconductor lasers: although semiconductor lasers are also solid-state devices, they are often classified in another category than solid-state lasers. Laser diodes produce wavelengths from 405 nm to 1550 nm. Low power laser diodes are used in laser pointers (1mW-5mW), laser printers, and CD/DVD players. The highest power industrial laser diodes with power up to 10kW are used in industry for cutting and welding. Vertical cavity surface-emitting lasers (VCSELs) are semiconductor lasers whose emission direction is perpendicular to the surface of the wafer. VCSEL devices typically have a more circular output beam than conventional laser diodes, and potentially could be much cheaper to manufacture. VECSELs are external-cavity VCSELs. Quantum cascade lasers are semiconductor lasers that have an active transition between energy sub-bands of an electron in a structure containing several quantum wells.

(3) Gas lasers and excimer lasers: The active media are gases which are typically excited with electrical discharges. Frequently used gases include CO₂, argon, and gas mixtures such as helium/neon. Common excimers are ArF, KrF, and F₂: typically a noble gas (rare gas) and a halogen. For instance, carbon dioxide lasers are used in industry for cutting and welding.

(4) Chemical lasers: They are powered by a chemical reaction, and can achieve high powers in continuous operation. They are used in industry for cutting and drilling. Common examples of chemical lasers are the chemical oxygen iodine laser (COIL), and the hydrogen fluoride laser and deuterium fluoride laser, both operating in mid infrared region.

(5) Dye lasers: they use an organic dye as the gain medium, usually as a liquid solution. Some of the dyes are fluorescein, coumarin, stilbene, umbelliferone, and tetracene.

(6) Fiber lasers are referred to as lasers with optical rare-earth doped fibers as gain media. Some lasers with a semiconductor gain medium and a fiber cavity are also called fiber lasers. The fiber laser will be focused on, as it is the core of this research. Common cavity configuration in fiber laser includes ring and linear cavity. The brief explanation is discussed as follows.

2.3.3 Linear Cavity

One of the most common types of laser cavity is known as Fabry Perot cavity. Historically, the subject of the laser resonators had its origin when (Dichie, 1958), (Prokhorov, 1958) and (Schawlow and Townes, 1958) independently proposed to use the Fabry Perot Interferometer as a laser resonator. The Fabry Perot cavity is formed by placing the gain medium between two high reflecting mirrors. In case of fiber laser, mirrors often coupled to the fiber ends to avoid diffraction losses. Mirroring can be formed by different material. For instance, fiber Bragg grating can act as a high reflectivity mirror. The use of two of such gratings results in all-fiber Fabry Perot cavity. Also, WDM coupler can as well utilize in such a way that the most of the pump power comes out of the port that is a part of the laser cavity. Figure 2.7 shows the all-fiber Fabry Perot configuration.

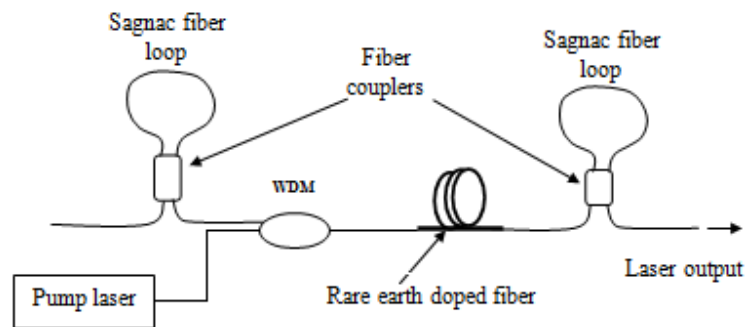


Figure 2.7:Schematic Diagram of All-Fiber Fabry-Perot Cavity

2.3.4 Ring Cavity

Ring cavities are often used to form unidirectional operations of a laser. In the case of fiber laser, an additional advantage is that a ring cavity can be made without using mirrors, resulting in all-fiber cavity. In the simplest design as shown in figure 2.8, the connecting arm of coupler 1 and 2 consist of ring resonator. The power is injected through port 3 while the laser output is obtained at port 4. The doped fiber used as a gain medium. In this research, instead of doped fiber as a gain medium, Single mode fiber is used, which proved to be cost effective as compared to doped fiber.

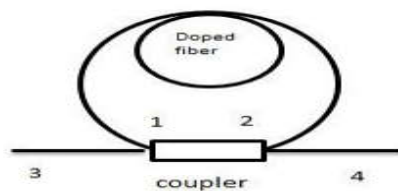


Figure 2.8:Schematic Diagram of All-Fiber Ring Cavity [IEEE Yang Zhang]

2.4 Fiber Based Laser

A fiber laser uses an active fiber as a gain medium in the ring or Fabry-Perot cavity configuration (Das and Chaboyer, 2009). The gain medium in general is a silica fiber doped with a rare-earth element. Some lasers with semiconductor gain medium and an undoped fiber resonator have also been called fiber lasers. They have wide applications in industry and medicine because of their unique characteristics such as an all-fiber design, compact size, cost-effectiveness in production and operation, and without re-alignment or external cooling. Fiber lasers are established as robust and reliable devices. Fiber lasers can also be divided into single-mode and multi-mode categories, depending on the modal structure of the laser.

2.4.1 Multi-wavelength Fiber laser

A fiber amplifier can be converted into a laser by placing it inside a cavity designed to provide optical feedback such lasers are called fiber lasers. In this kind of laser, there are optical fibers that act as gain media such as erbium or ytterbium doped fibers among others. Therefore increase the gain of these fiber amplifiers causes lasing to occur and more lasing lines to be generated. Multi-wavelength fiber laser includes but not limited to Erbium doped fiber multi-wavelength Brillouin fiber laser (MWEDFL), Brillouin fiber laser (MWBFL), Brillouin erbium fiber laser (MWBEFL) and Brillouin Raman fiber laser (MWBRL).

2.4.1.1 Erbium Doped Fiber Laser

The use of erbium doped fiber amplifiers is commonly used as a gain media due to their high gain with broad bandwidth, low threshold, high power conversion efficiency and compatibility with fiber communication systems. Then, the number of lasing wavelength equivalent to the output channels generated is at the same time very important and it is directly

depends on the system transmission capacity. However, the homogenous nature of the erbium normally poses a major barrier to obtain a stable multi-wavelength emission at room temperature (Desurvire, 2002). Scientists observed that insertion of an intra-cavity filter associated with an acousto-optic frequency shifter in the laser cavity, multi-wavelength lasing was possible (Karasek and Bellemare, 2000). This frequency shift forbids the existence of a stationary state in the cavity. By cooling the gain in liquid nitrogen at 77K, homogenous broadening of erbium is largely reduced. Meanwhile, this method is inconvenient and it may impact the device durability leading to complexity in component configuration, so it is not easily integrated in industrial system. In (Prokhorov, 1958), a single piece of erbium-doped fiber is used to provide an inhomogeneous gain medium through macroscopic spatial burning. As the available gain at each lasing wavelength is partially decoupled from the others, simultaneous operation of several single frequency modes can be reported.

2.4.1.2 Brillouin Fiber Laser

This is a single gain medium fiber laser and it is generated by cascading stimulated Brillouin scattering as a simple, accurate and consistent method with flexible wavelength tuning (Shiraziet. al., 2008; Buttneret. al, 2012). In this case single mode fiber is used in cavity formation where multiple wavelength lasing occurs. Brillouin Stokes power is dependent on BP power in a SBS process. So, it is customary to use hybrid gains such as Brillouin-erbium and Brillouin Raman gains to increase the number of Brillouin Stokes line generated in SBS process in MWBEFL and MBRFLs respectively (Shee et. al, 2011; Tang et. al, 2011; Shirazi and Biglary, 2012; Ali et. al, 2013; Shirazi et. al, 2013; Shirazi et al., 2014)

2.4.1.3 Brillouin Raman Fiber Laser

The basic concept of MBRFL is the same as in MBEFL in the aspect of combination two gain inside the cavity but the difference here comes from using nonlinear gain represented by Raman fiber amplifier (RFA) instead of using linear Erbium doped fiber (EDF) gain. In other words the MBRFL is the combination between two nonlinear gain media, inside the SMF (Zamzuri et. al., 2009; Kamaljit et al., 2010). The principle of multi-wavelength generation can be explained by coupled interaction of three nonlinear scattering processes. As the power of Raman pump (R_p) lasers increase, injected Brillouin pump (BP) power exceed the Brillouin threshold. The feedback for multiple Stokes generation is provided by frequency shifted Brillouin scattering, and frequency un-shifted Rayleigh scattering and Raman gain is provided both for the amplification of the Brillouin and Rayleigh scattered power (Min et al., 2001). The generation of Brillouin Stokes lines (BSL) occurs when the BP reaches the SBS threshold. That BSL is then amplified by Raman amplification as it propagates in the opposite direction to the BP propagation direction.

During its propagation, it generates a second-order Brillouin Stokes line propagating in the same direction as the BP. This process continues as long as the particular higher-order Stokes line has a round-trip gain equal to the cavity loss. The round-trip oscillation in the laser cavity is formed by a mirror at each end of the laser structure. These mirrors are used to reflect Stokes lines as well as the residual R_p (Zamzuri et. al, 2009). Raman amplification in MWRFL has a wide gain bandwidth and the generation of Brillouin Stokes is higher compare to its counterpart of MWBEFL but it requires a relatively long non-linear fiber due to the nature of its amplification.

2.4.1.4 Brillouin/Erbium Fiber Laser

Instead of using only single gain medium such as the rare earth doped fiber, a BEFL employs two gain media, namely from the non-linear gain in SMF and the linear gain from the EDF. A ring cavity of BEFL is shown in Figure 2.9. When the SMF is pumped with a narrow-line width laser source which is also known as a Brillouin pump (BP), a Stokes-shifted wave is generated in the reverse direction which is then amplified by the EDF. The potential for this type of laser is that the wavelength of the resulting laser can be determined very accurately due to the known frequency shift from the pump signal. By pumping the EDF with a 1480 or 980 nm laser diode (in most cases) gain can be produced to overcome the resonator loss. When the BP wavelength is set close to the maximum gain produced by the EDF, lasing will occur at the Stokes-shifted wavelength.

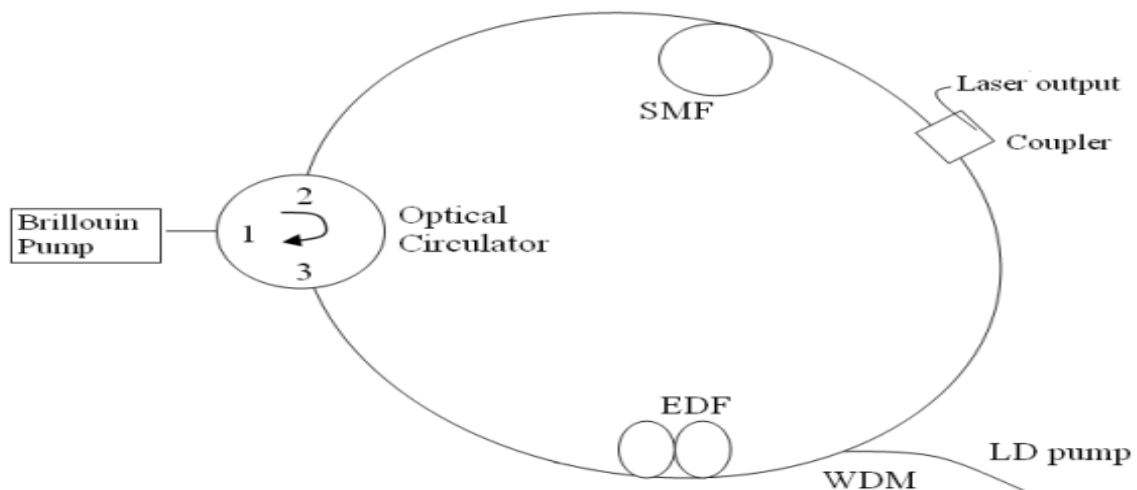


Figure 2.9: Schematics diagram of the BEFL configuration

Figure 2.10 depicts schematically the BEFL operation. The broad-band gain with the maximum peak wavelength of λ is generated by the EDF, while narrow-band gain is generated from the

SBS process in the SMS at a wavelength of z as shown in Figure 2.10. If the total gain of wavelength z is greater than that of wavelength x and is equal to the threshold gain of g_{th} , then lasing actions will commence due to the combination of the two gain media.

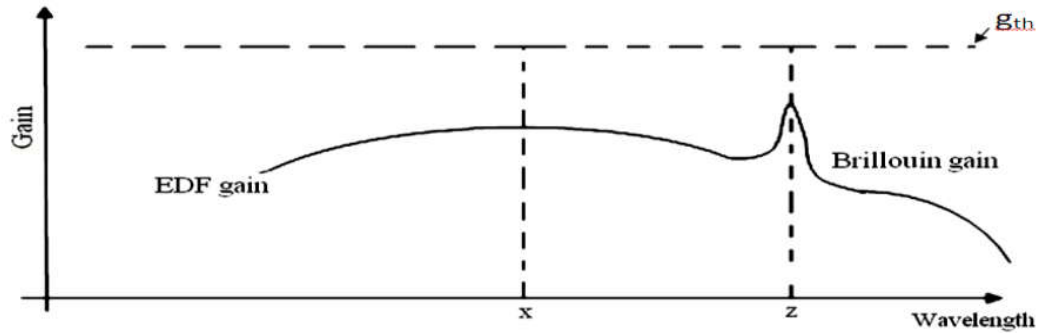


Figure 2.10: Schematics diagram of BEFL operation

Since Brillouin gain is relatively small as compared to the EDF gain, the BEFL must operate at a wavelength at which EDFL would operate without Brillouin gain. BEFL operates in a manner different to that of EDFL and BFL in which it combines both the two characteristics. The wavelength operation is determined from the Stokes shift frequency, which is to BFL, and above threshold, the characteristics are similar to those of EDFL in which most of the BEFL power in the output is extracted from laser diode (LD) pump.

The conversion efficiency of the laser can be determined by the amount of pump power that is converted to output. As the BEFL comprises of two gain media, thus each gain media will contribute to the pump power and the overall conversion efficiency can be written as (Stepanov and Cowle, 1997b)

$$\eta(I_{(E)}, I_{(B)}) = \frac{I_{out}}{I_B + I_E} \quad (2.5) \text{ Where}$$

I_{out} , I_B , I_E are the laser output, EDF pump and BP intensities. The output intensity depends on the pumping level of the EDF and SMF and it can be written as follows:

$$I_{(out)} = \eta_E I_{(E)} + \eta_B I_{(B)} + \eta_{EB} I_{(E)} I_{(B)} + I_{(sat)} \ln(1 - R) \quad (2.6)$$

Where $I_{(sat)}$ is the saturation intensity, R is the coupler ratio, $\eta_E, \eta_B, \eta_{EB}$ are erbium, Brillouin efficiency and cross efficiency of erbium/Brillouin respectively. Various BEFL schemes will be thoroughly studied.

2.5 Previous Works on MWBEFL

Many works have been reported on the multi-wavelength fiber laser, for instance (Cowle et al., 1996) proposed a hybrid gain media for the fiber laser operating at room temperature. The hybrid gain media consisted of respectively Brillouin gain and erbium doped fiber amplifier (EDFA) gain termed multi-wavelength Brillouin erbium fiber laser (MWBEFL). The Brillouin gain was triggered by an optical pump source with a narrow line-width. SBS effect generated Brillouin signals in the optical spectra. The frequency difference between Brillouin signals was established due to acoustic velocity in the fiber. In a fiber scheme with such a hybrid gain media, simultaneous operation of multiple wavelengths with a channel spacing of 0.0824nm was realized by continuously seeding the Brillouin signals (Stepanov and Cowle, 1997a).

Harun et al, 2002 reported BEFL L-band Brillouin-Erbium fiber laser. The BEFL operates around 1598-1612nm. The EDFA of 50-m long is used to amplify the Brillouin gain. A 10GHz spacing multiple wavelengths were produced by two 3dB couplers joined in reverse – S arrangement in the resonator as shown in figure 2.11. The portion of BEFL signal was feedback

into SMF to seed a cascaded BEFL. 20 stable lines including the Anti-stokes lines were obtained as shown in figure 2.12. This 20-channels can be tuned at 14nm within L-band range of 1598-1612nm.

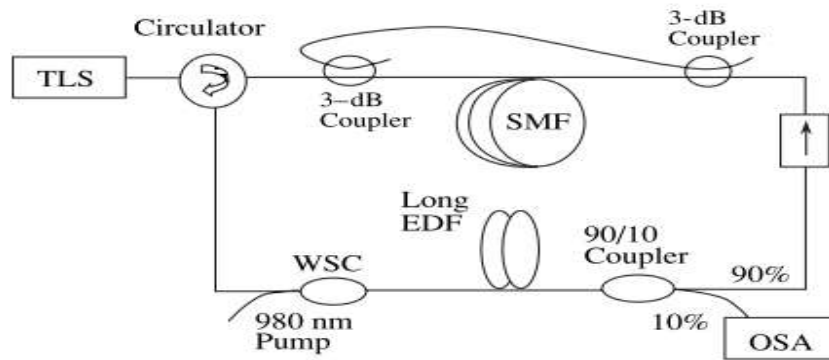


Figure 2.11: Experimental setup of the internal cascade technique used to generate multiple wavelengths.

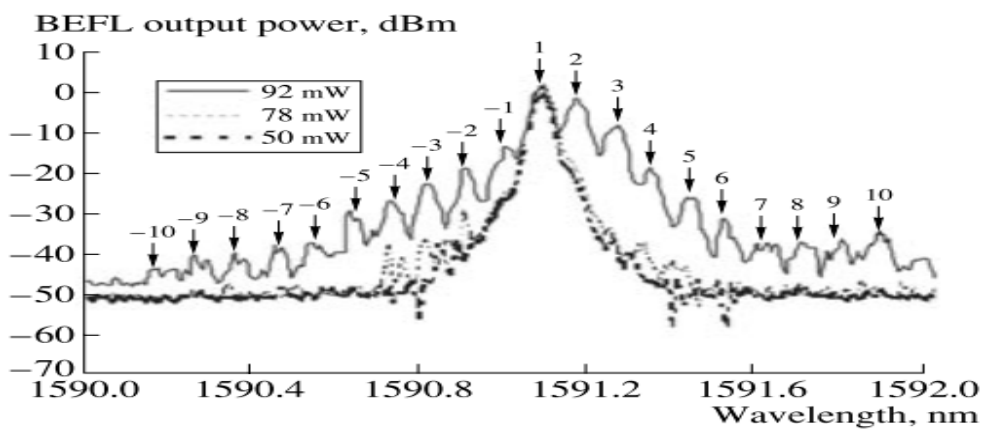


Figure 2.12: Spectrum of the BEFL for various 980 nm pump power

Haddud et al., 2005 reported 24-line Brillouin fiber laser utilizing fabry Perot cavity in L-band. The configuration utilized a fabry perot cavity formed by the loop mirrors as shown in figure 2.13. 24-lines of Brillouin Stokes with the line spacing of 10GHz are obtained in L-band region of 1597nm BP wavelength with 0.18mW total output power, the result of which is shown in figure 2.14. This laser system can be tuned over a tuning range of 10 nm.

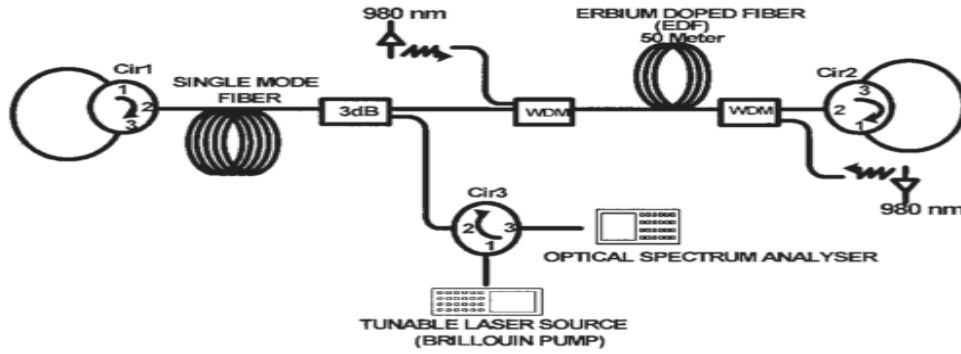


Figure 2.13: Experimental setup of a multi-wavelength BEFL utilizing a Fabry–Perot resonator in the L-band region

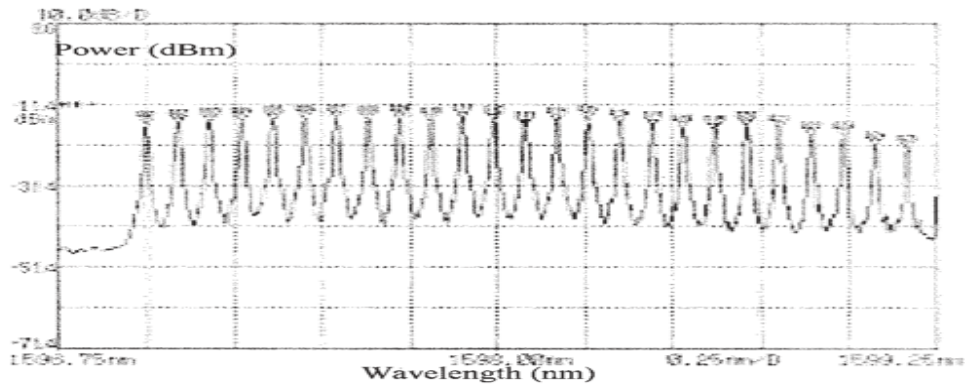


Figure 2.14: Optical spectrum of 24 cascaded Stokes with BP power set at 0.18mW

Mahdi et al., 2007 reported Enhancement of multi-wavelength generation in the L-band by using a novel Brillouin-Erbium fiber laser with a passive EDF booster section as shown in figure 2.15. 28 stable output channels with a spacing of 0.089 nm can be generated as shown in figure2.16.

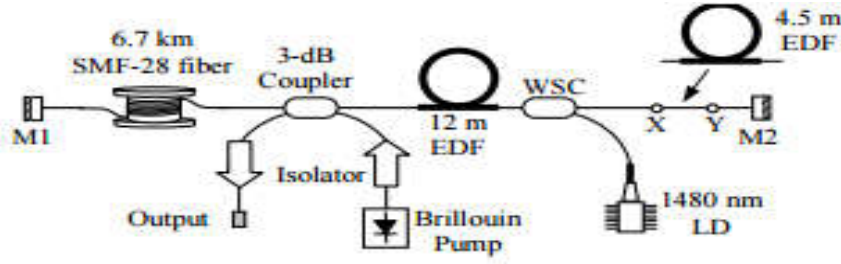


Figure 2.15: Experimental setup of a linear cavity multi-wavelength L-band Brillouin-Erbium comb fiber laser

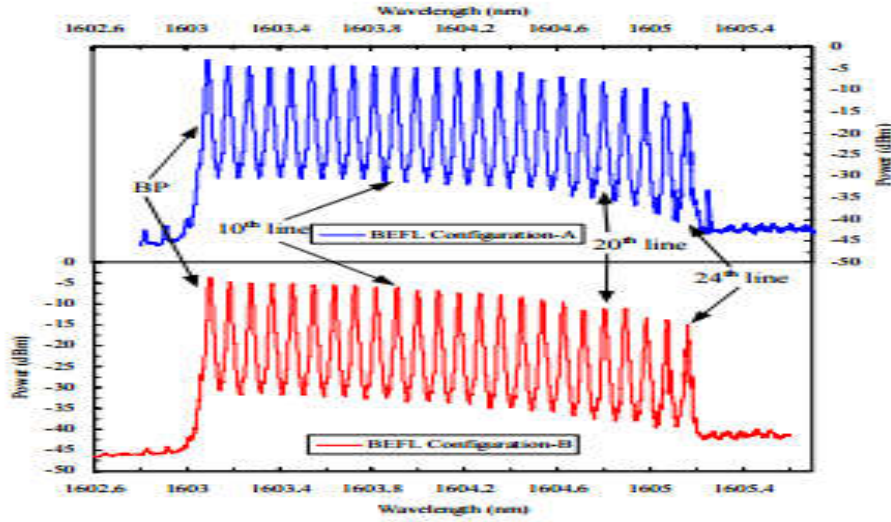


Figure 2.16: Output spectrum from both BEFL configurations at pump power of 73mW, BP power and wavelength are set at 1.1mW and 1603.1 nm respectively.

Al-Mansoori and Malin, 2009 demonstrated L-Band MWBEFL utilizing double pass BP pre-amplified method. The configuration is as shown in figure 2.17. The threshold power of about 15.9mW generates the first Stokes signal and maximum of 30-channel at 10GHz spacing between adjacent channels tuned at 14nm of BP wavelength. The 1480nm pump and BP power of 40 and 0.035mW used to generate the maximum channels as shown in figure 2.18.

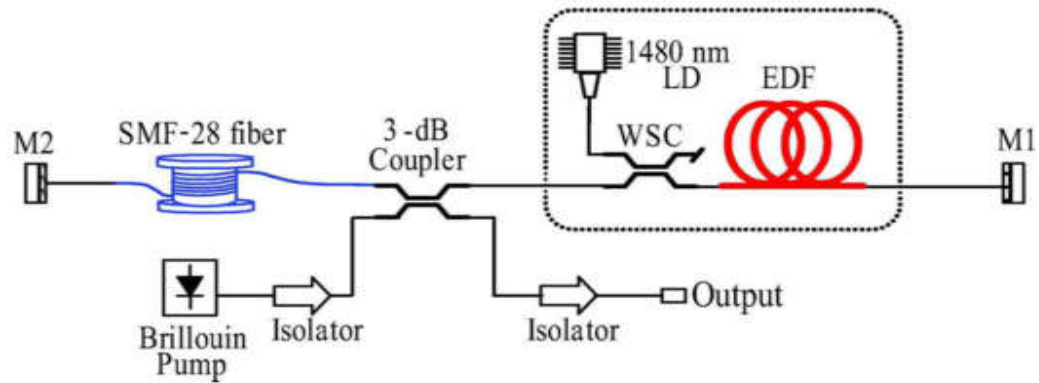


Figure 2.17: Schematic diagram of a linear cavity MWBEFL with double-pass BP pre-amplified technique

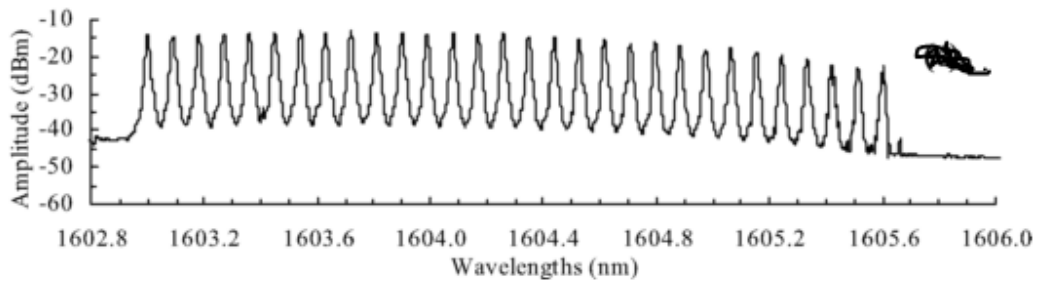


Figure 2.18: Output spectrum at different BP and 1480 nm pump powers at 0.035mW and 40mW

Al-Mansoori and Mahdi, 2011 recently reported broadly tunable L-band MWBEFL utilizing nonlinear amplified loop mirror filter (AFLMF). The configuration is as shown in figure 2.19. 24 stable output channels at 10GHz spacing between adjacent channels are generated with the maximum of 100mW 1480 nm pump and 1.1mW Brillouin pump power respectively as depicted in figure 2.20. All these 24-channels can be tuned over 40nm L-band range between 1570-1610nm.

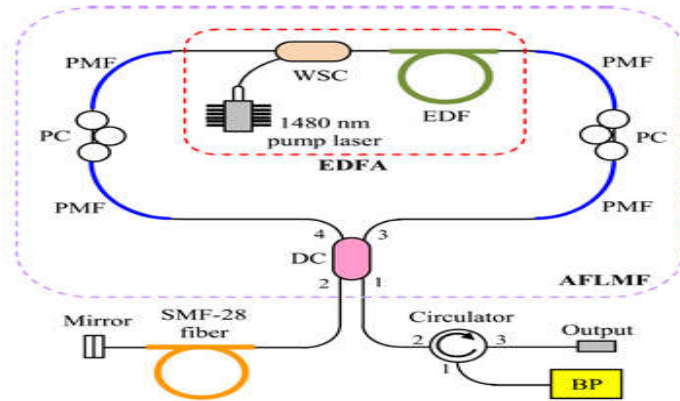


Figure 2.19: Experimental setup of multi-wavelength BEFL utilizing nonlinear AFLMF.

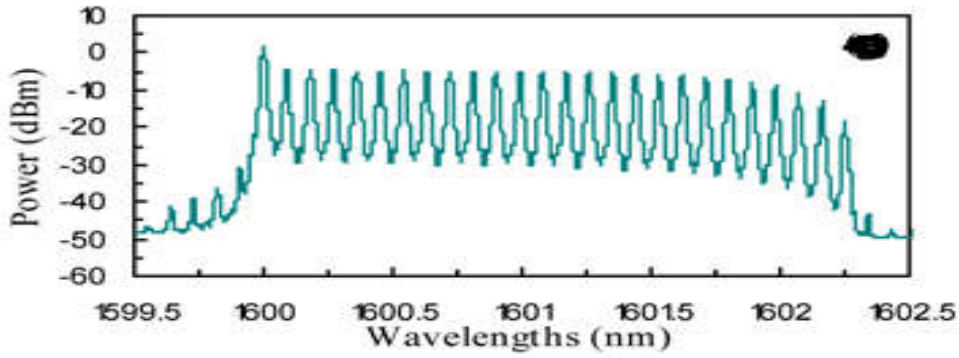


Figure 2.20: 24-Stokes Channel Output spectra of MWBEFL utilizing nonlinear AFLMF

Parvizi et al., 2013, also reported 20GHz optical combs in a Brillouin erbium fiber laser. The configuration utilized a four port circulator that provide isolation and circulation of odd-order Brillouin Stokes signals through the 10Km long zero dispersion shifted fiber as a Brillouin gain medium in the ring cavity as shown in figure 2.21. About 15 channels are generated with 0.173nm wavelength spacing as depicted in figure 2.22. The tuning range obtained as 10nm from the range of 1552nm to 1562nm.

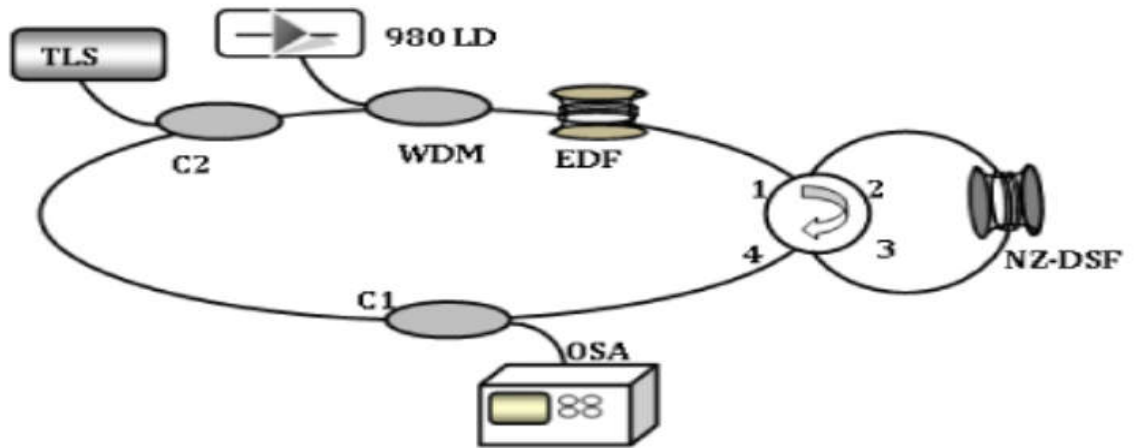


Figure 2.21: Configuration of the multi-wavelength BEFL with double spacing

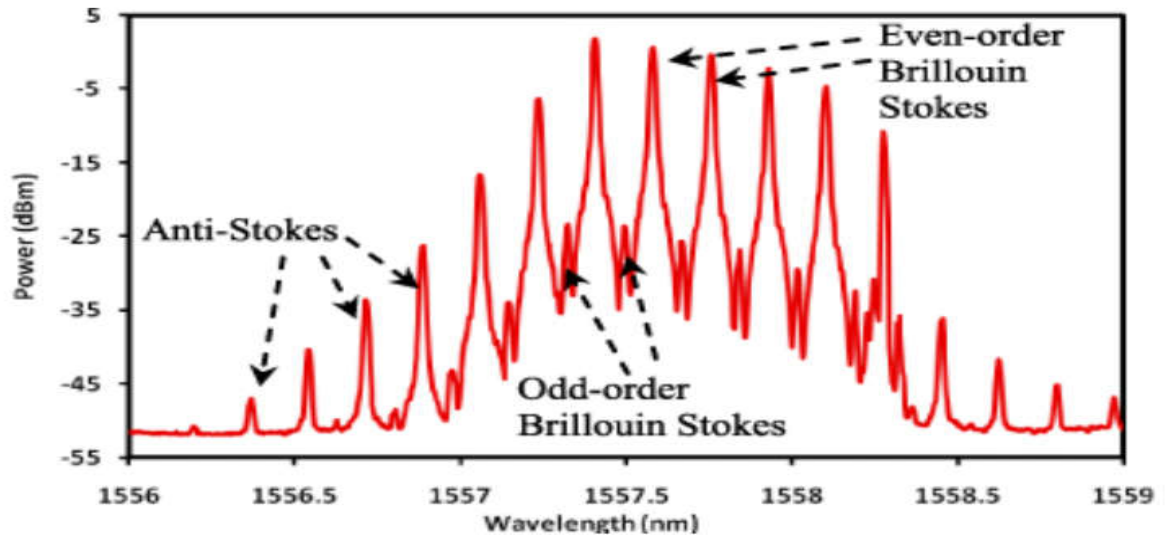


Figure 2.22: Output spectrum of the MWBEFL with BP power of 3dBm and 50mW pump power

Conclusively, in order to show the improvement of this research over existing works, the achievement and limitation of the previous works need to be marked out. This is summarized as shown in table 2.1

Table 2.1: Summary of previous work reviewed

Author Name and Year	Types of Fiber Laser	Number of Channel	Channel Spacing (GHz)	Tuning Range (nm)	Band	Limitation
Harun et al., 2002	MWBEFL	20	10	-	L	Narrow spacing and low channel
Haddud et al., 2005	MWBEFL	24	10	-	L	Narrow spacing and low channel
Mahdi et al., 2007	MWBEFL	28	10	-	L	Narrow spacing
Al-Mansoori and Malin, 2009	MWBEFL	30	10	-	L	Narrow spacing
Al-Mansoori and Mahdi, 2011	MWBEFL	24	10	-	L	Narrow spacing and low channel
Parvizi et al., 2013	MWBEFL	15	20	10	C	Low channel

Therefore, in most of the previous works reviewed there are limitations specifically, a fixed narrow channel spacing between the adjacent channels, low output channels and tuning range as can be clearly seen in table 2.1 and these performance parameters need to be improved for the MWBEFL laser to be well suitable to be used in many application especially in DWDM system. Therefore in this research, a structure of MWBEFL with adjustable spacing between adjacent channels is considered. This structure contains comb filter termed delay interferometer which provides control over the spacing between adjacent channels. This means that, more spacing can be allowed between the channels and with proper adjustment of EDFA gain and Brillouin pump power, large number of channels with high tuning range can be obtained.

CHAPTER THREE

METHODOLOGY

3.1 Introduction

This chapter presents the methodology of this research. The experimental setup and principle of operation of MWBEFL configuration employed in this research were discussed in details. Lastly, BEFL parameters under study (design parameters and performance parameters) were briefly explained in order to have a better understanding of the construction of the multi-wavelength BEFLs.

3.2 Principle of Operation of the Simulation Set Up

The simulation set up of the L-Band Brillouin Erbium fiber laser utilizing Delay interferometer for channel spacing is depicted in Figure 3.2. The set up consists of Continuous wave Laser and EDFA as Brillouin pump at wavelength of 1600nm. Erbium Doped Fiber Amplifier (EDFA) is fixed at gain of 10dB, Delay Interferometer at wavelength of 1550nm and time delay of 0.05ns, Optical Circulator, Loop Control, Ideal Isolator, Single mode fiber (SMF) of 25km length, attenuation of 25dB, 16.75ps/nm/km of dispersion and Optical Spectrum Analyzer (OSA) of 0.01nm resolution bandwidth. The Circuit is implemented in optisystem optical system simulation software. The continuous wave laser amplified by Erbium Doped Fiber Amplifier is used as Brillouin pump because in order to experience SBS effect, a higher BP power is required and the amplified signal is directed to the Delay Interferometer. The signal is passing into the circulator and into the Single mode fiber. Then the cavity is formed. When the total gains i.e. Brillouin gain and EDFA gain in the cavity is equal to the cavity loss, lasing starts in the cavity. The main purpose of EDFA gain is to amplify the Brillouin gain in order to compensate for the loss in the laser cavity, so that SBS effect can be initiated and also to increase

the laser output power. The lasing continues, provided the gain in the cavity is equal or greater than the cavity loss. The channel spacing between the Stokes signals or between anti-stokes signals is determined by the time delay of delay Interferometer. The output waves generated is measured by optical spectrum analyzer connected to the Isolator and circulator. The output Signal measured after isolator is referred to as Transmitted Signal while the output signal at port 3 of circulator termed reflected signal.

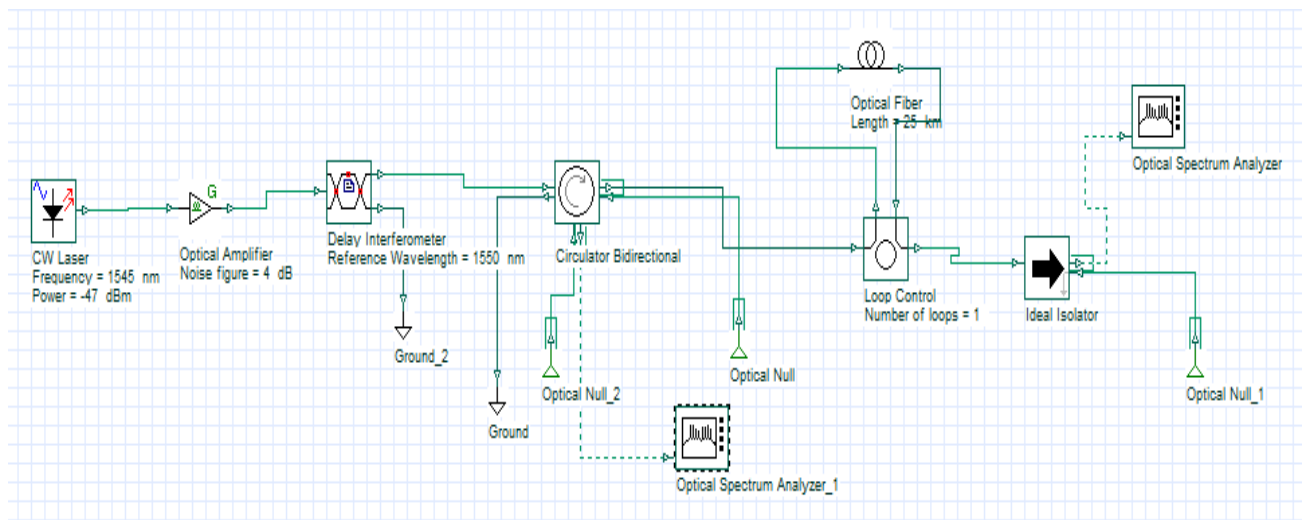


Fig.3.1:MWBEFL simulation set up in optisystem

3.3Optisystem Library Components Used in MWBEFL Design

The configuration of this type of fiber laser consist of Brillouin pump power made up of continuous wave laser and EDFA mainly put in place to produce high gain for SBS process to be initiated. The other components used in this research includes Comb filter delay Interferometer, single mode fiber (SMF), loop control, Isolator, optical spectrum analyzer (OSA), Power meter, WDM analyzer. All the components used here are picked from the components library of optisystem software. The details of the components are individually discussed here.

3.3.1 Continuous wave Laser

Lasers are used for converting electrical current into light. Laser commonly used in optical communication because it has several advantages. Some important features of the CW laser includes small size, long life and can be modulated easily. Light emitting diode (LED) is also useful but laser has the following advantages on LED diodes. The speed of laser is faster and provides high bandwidth and also spectral width provided by the laser is narrow as compare to LED. In this research the CW laser with assistance of EDFA as an amplifier is considered as a tunable laser source that is used as Brillouin pump.

3.3.2 Brillouin Pump

The Brillouin pump used in this research consists of CW laser and EDFA to produce high gain so that SBS process will be initiated. The Brillouin pump is also an important parameter in determination of tuning range as Brillouin pump wavelength can be tuned at a very wide range. In this research wavelength is tuned through the entire L-band of 1565nm to 1625nm and since number of output generated depends on the total output power, the maximum output number produced is considered in determination of tuning range.

3.3.3 Optical Circulator

An optical circulator is a nonreciprocal multiport passive device that directs light sequentially from port to port in only one direction. The operation of a circulator is similar to that of an isolator except that its construction is more complex. Circulator can either be three or four ports but three ports circulator is commonly used. The structure of three ports circulator is shown

in figure 3.3. Input on port 1 is sent out on port 2, an input on port 2 is sent out on port 3 and an input on port 3 is sent out on port 1.

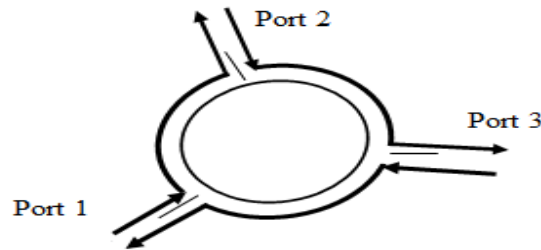


Figure 3.2: Schematic Diagram of Three Port Circulator

More so, circulator has low insertion loss, high isolation over a wide wavelength range, minimal polarization dependent loss (PDL), and low polarization mode dispersion (PMD). The circulator use in this simulation is picked from component library of optisystem optical software with detail specification as shown in table 3.1

Table 3.1: Details specification of three port circulator used

Parameter	Unit	Value
Operating wavelength	Nm	1550
Bandwidth	Nm	130
Insertion loss	dB	0
Maximum insertion loss	dB	3
Isolation	dB	55
Min. Isolation	dB	45
Return loss	dB	65
Min. Return loss	dB	60
Noise threshold	dB	-100
Noise dynamic	dB	3

3.3.4 Optical Isolator

Optical isolators are devices that allow light to pass through them in only one direction. This is important in a number of instances to prevent scattered or reflected light from travelling in the reverse direction. One common application of an optical isolator is to keep such light from entering a laser diode and possibly causing instabilities in the optical output. The details chosen

for isolator in this research is as the same as that chosen for the optical circulator as shown in table 3.1.

3.3.5 Optical Amplifier

Optical amplifier enables the design of amplifiers, including EDFAs that consider pre-defined operational conditions. This means that expected gain, Noise Figure and amplifier output power can be specified. The amplifier presents the same facilities as a block box model, which enables the operation mode with gain control, power control, or simulation under saturated conditions. It defines the expected amplifier performance as well. In this project, the amplifier is operated in expected gain mode.

3.3.6 Delay Interferometer

The DI which is fabricated using Si-SiO₂ waveguide technology has two arms with a 25ps time delay between the two arms (Chen et al, 2009). The light is split into two beams, and, at the output of DI, two beams of optical signals with the phase difference (corresponding to 25ps delay) recombine and interferes with each other. The optical intensity at the DI output can be given as shown in equation (3.1) (Chen et al, 2009)

$$I_{out}(\lambda) = I_{up}(\lambda) + I_{low}(\lambda) + 2\sqrt{I_{up}(\lambda) * I_{low}(\lambda)} \cos \Delta \theta \quad (3.1)$$

Where, $\theta = 2\pi C * t / \lambda$

Where, I_{up} and I_{low} are intensity of two beams travelling along the two arms of the DI, t is the travel time delay between the two arms; C is the speed of light in vacuum and λ is the wavelength of the optical signal. The DI acts as a comb filter which makes the wavelengths that match the peaks of the comb oscillate when it is in a laser cavity. The wavelength spacing

between two adjacent transmission peaks is 0.32 nm for $t = 25$ ps. The line width of the peaks is reduced for the two trip transmission (equivalent to two cascaded DIs). Multiple transmissions through identical DIs will further reduce the line width of the transmission peaks. By increasing the time delay of the delay interferometer the wavelength spacing is reduced and increase the number of wavelength channel. The delay interferometer use in this study is picked from the library component of Optisystem optical software, the parameters specified for the delay interferometer in this study is shown in table 3.2

Table 3.2: Details specification of comb filter delay interferometer used

Parameter	Unit	Value
Reference wavelength	Nm	1550
PDF	dB	30
Additional loss	dB	0
Insertion loss	dB	30
PDL	dB	0.05

3.4 Brillouin Fiber Laser Parameters

In this study, the parameters of the Brillouin fiber laser are studied. The parameters refer to includes the input and output parameters. The input parameters refer to as the design parameters that can be adjusted, so that the best performance of the laser system can be obtained. The input parameters considered in this simulation research includes EDFA gain, Brillouin pump power and wavelength and time delay. The output parameters can be defined as the performance measure parameters obtained as a result of variation in design parameters. The performance parameters considered in this study includes threshold power, peak power of the Stokes, number of output channels, OSNR, channel spacing and tuning range.

3.4.1 Design Parameters

The design parameters refer to as input parameters of the Brillouin fiber laser that alter for the purpose of the laser optimization. The design parameter considered in this study includes EDFA gain, Brillouin pump power and wavelength and time delay of the comb filter called delay interferometer. The modification of the laser as a result of change in any of these parameters result in changes the output performance of the laser. The details about these parameters are discussed as follows.

3.4.1.1 Brillouin Pump Power

No SBS takes place without the Brillouin pump power and Stokes cannot be generated. The higher Brillouin gain in the cavity as a result of high Brillouin pump power provides sufficient signal power for higher order Stokes signals to pump the SMF and maintain cascading process of the multiple channels. Increase in Brillouin pump power leads to increase in Stokes peak power due to high Brillouin gain in the cavity and that the peak power of each subsequent Stokes is generated with the energy of the previous Stokes due to the fact that, the input power conversion to Brillouin Stokes from Brillouin pump is always less than the actual input power injected because of pump depletion. The Brillouin pump source used throughout the whole works of this study was taken from continuous wave laser diodes whose output is amplified by optical amplifier (EDFA).

3.4.1.2 Brillouin Pump Wavelength

Brillouin pump wavelength is a very useful parameter in performance optimization of the Brillouin fiber laser. In order to optimize the Brillouin fiber laser, Brillouin wavelength must be

tuned to the peak in which there is absence of free lasing cavity mode where maximum output power with high output channel is produced. In case of laser that utilized doped fiber as a gain medium, BP wavelength must be tuned to the Erbium doped fiber laser peak gain wavelength for the efficient conversion of the gain. Generation of the maximum output channel depends on the positioning of Brillouin pump at the right wavelength. The Brillouin pump wavelength in this study is tuned within the L-band ranges of 1565nm to 1625 nm.

3.4.1.3 EDFA Gain

Optical gain is realized when the laser medium is pumped to achieve population inversion. Increasing the EDFA gain cause signal amplification provided the number of the erbium ion in the core has not reached the maximum limit. Therefore the gain of the EDFA is limited by the fact that there are a limited number of erbium ions in the core. Increasing the pump power beyond the point where all ions are excited cannot produce more gains and thus saturation occurs. Gain is the ratio of the amplifier output signal power to the input signal power. This is mathematically expressed as in equations 3.2 and 3.3.

The gain is given as shown in equation

$$G = P_{s,out}/P_{s,in} \leq (\lambda_p/\lambda_s)P_{p,in}/P_{s,in} \quad (3.2)$$

The maximum possible gain is the obtained as shown in equation

$$G = P_{s,out}/P_{s,in} \leq 1 + (\lambda_p/\lambda_s)P_{p,in}/P_{s,in} \quad (3.3)$$

Where, $P_{s,out}$, $P_{s,in}$ and $P_{p,in}$ are the output power, input power of signal and pump power respectively. Then λ_p and λ_s are pump and signal wavelengths.

3.4.1.4 Time Delay

The time delay is the travel delay between the two arms of delay interferometer. The time delay of delay interferometer can be compared as inversely related to the frequency and based on the time delay, the shift space between the channels can be determined. For instance time delay ($t = 25\text{ps}$) between two polarization components provides a one bit time shift which corresponds to the frequency shift of 40GHz. Multiple transmission between the two beam at the output of DI causes the reduction in the channel spacing but increasing the number of output channel.

3.4.2 Performance parameters

The performance parameter as discussed earlier is the output parameters used to optimize or measure the performance of the Brillouin fiber laser. In this thesis various performance parameters were considered to evaluate and represent the working conditions of the multi-wavelength BFL. The performance parameters are: threshold power, peak power of the channels (Stokes and anti-Stokes signal), number of output channels (Stokes and anti-Stokes signal), channel spacing between two adjacent channels, OSNR and tuning range.

3.4.2.1 The Output Channel Peak Power

The peak power of the individual channel (Stokes or anti-Stokes signal) is determined from the optical spectrum analyzer as the signals peak power and is termed as the Stokes or anti-Stokes signal peak power. The peak power for all orders of the Stokes signal in general, increases when the pump power or EDFA gain is increased. The total peak power is the highest output power that a fiber laser can achieve at a fixed value of input power. The peak power of the Stokes or anti-Stokes signal is always lower than that of the previous one. This is obvious since

the conversion from a Brillouin pump signal to the Stokes signal is always less than unity. In addition, the Stokes or anti-Stokes signal peak power is higher at a higher Brillouin pump power or EDFA gain. The evaluation of the peak power and the total output power of the Stokes or anti-Stokes signal will be given in the chapter chapter four.

3.4.2.2 Threshold Power

Based on the arrangement in MWBEFL laser structure, the EDFA is operated in a gain mode rather than in a power mode. Therefore the lasing threshold is defined as the amount of EDFA gain that prompted lasing at a fixed Brillouin pump power in the cavity system of multi-wavelength Brillouin fiber laser. The indication of lasing is the appearance of first Stokes signal. The Brillouin pump power causes SBS effect as it serves as launch power to initiate this nonlinear effect. BEFL threshold is determined by the requirement that the total gain (linear EDFA gain and nonlinear Brillouin gain) should be equal to the total cavity loss. The threshold is measured by the gain of the EDFA while Brillouin pump is fixed at a certain value. This is done at a point when the first Stokes signal starts appearing. Once the threshold above, the BEFL output power and the number of output channels (Stokes and anti-Stokes signals) increases in tandem with EDFA gain. In multi-wavelength BEFL system, multiple number of Stokes signal is generated and therefore there are a series of threshold values to be determined in this system according to the order of Stokes as this has been demonstrated and analyzed in the next chapter.

3.4.2.4 Number of Channel Generated (Stokes and Anti-Stokes signal)

The ultimate goal of the Brillouin fiber laser is the ability to produce high output channel that can be tuned at a wider range. Number of channel (Stokes and anti-Stokes signal) increases

with increase in the Brillouin pump power or EDFA gain and vice versa. The limitation of the output channels includes the presence of free lasing cavity mode and depletion of the pump power in the cavity which make the higher order signal not lasing. Also at much higher Brillouin pump power with optimum EDFA gain, the number of lasing line is reducing. This is due to the fact that at higher BP EDFA is forced to operate in deep saturation region and drastically reduce the EDFA gain.

3.4.2.5 Tuning Range

The capability of wavelength tuning range is a key parameter of a tunable Brillouin fiber laser. Tuning range of the multi-wavelength BFL is defined as the range of Brillouin pump wavelength in the absent of self lasing cavity modes. Due to the nature of the Stokes signal in a multi-wavelength BFL system, just by tuning the Brillouin pump signal the entire Stokes signal shifts simultaneously according to the range tuned. Tuning range depends on total output power as a result of EDFA gain and Brillouin pump power to capture the cavity loss. A wider lasing gain would generally allow a wider tuning range besides allowing higher order Stokes shifted signal to lase but at the same time giving rise to more cavity modes to compete with these Stokes shifted signal. The tuning range is studied in this research by tuning the BP wavelength within the range of L-band (1565nm-1625nm) and considered the number of output channel generated with the total output power.

3.4.2.6 Optical Signal to Noise Ratio (OSNR)

OSNR is the key performance parameters in optical network that predict the bit error rate (BER) of the system. OSNR is performed by comparing the peak power of the generated channels with the highest noise level. The noise power and channel peak power in this study are

measured by DWDM analyzer and Optical spectrum analyzer respectively. The OSNR increases as the peak power of the channel increases. EDFA gain increment to boost the Brillouin gain lead to decrease in OSNR, which implies that, the higher the EDFA gain, the lower will be the OSNR and vice versa.

3.5 Conclusion

The design of a controlled spaced channel MWBEFL are based on simulation carried out in simulation environment of optisystem optical simulation software. Delay interferometer is utilized to have control over the spacing between adjacent channels. The principle of operation of this MWBEFL was properly discussed. Brief explanations on the BEFL parameters and components have been given in order to have a better understanding of the construction of the MWBEFLs. The characterization of the design parameter and its effect on the performance parameters will be discussed in the next chapter.

CHAPTER FOUR

RESULT AND DISCUSSIONS

4.1 Introduction

This chapter presents the results of the simulation of L-band MWBEFL with adjustable spacing between the adjacent channels through optisystem optical simulation software. The results of the effect of input parameters such as EDFA gain, time delay of delay interferometer, Brillouin pump power and wavelength on performance parameters are properly analyzed where necessary. The performance parameters considered in this study includes threshold power, Stokes and anti-Stokes peak power, wavelength tunability, total output power, channel spacing, number of Stokes and anti-Stokes generated. The measuring tools use in this simulation includes optical spectrum analyzer, optical power meter and DWDM analyzer

4.2 Effect of EDFA Gain

The EDFA gain in this multi-wavelength laser configuration is meant to amplify the Brillouin pump power, because in real life experiment, high power Brillouin pump may not be available, so EDFA is positioned immediately after the Brillouin pump power for pump power amplification. Therefore, where low Brillouin pump power is used, the EDFA gain or pump power determines the lasing condition of the system. The study of the effect of EDFA gain was performed at a fixed low Brillouin pump power of -65dBm and Brillouin wavelength of 1600nm. Then, the threshold power, Stokes signal peak power and numbers of Stokes signal were studied while varying EDFA gain.

4.2.1 The Effect of EDFA Gain on Threshold

In this case, the threshold is defined as the amount of EDFA gain that prompted lasing at a fixed Brillouin pump power in the cavity system of multi-wavelength Brillouin fiber laser. The indication of lasing is the appearance of first Stokes signal. The threshold of this multi-wavelength laser was studied at a fixed low Brillouin pump power at -65dBm and Brillouin wavelength at 1600nm while varying the EDFA gain. Figure 4.1 and figure 4.2 show the lasing demonstration of this multi-wavelength laser. In figure 4.1, the EDFA gain was input as 5dB and there is no appearance of Stokes signal but by increasing the EDFA gain to 10dB, first Stokes signal with 0.16nm wavelength channel spacing equivalent to frequency spacing of 20GHz (double spacing) appeared as depicted in figure 4.2.

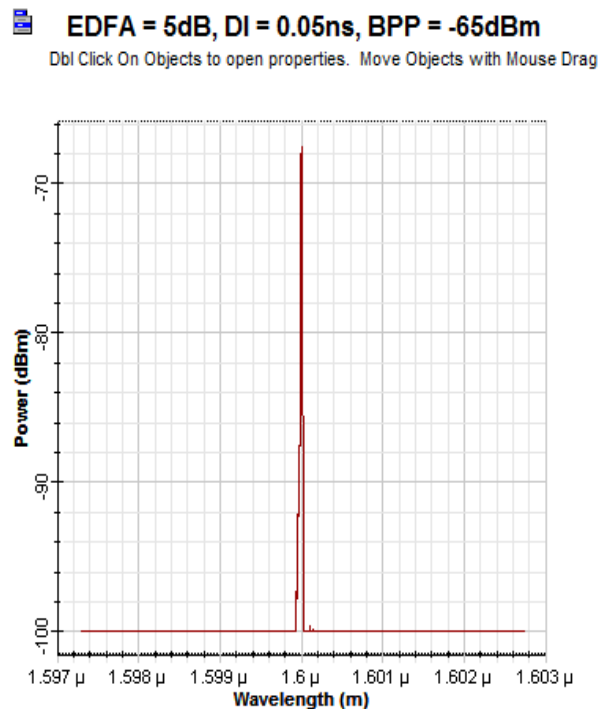


Figure 4.1: Output spectrum of no lasing condition in the cavity at EDFA gain of 5dBm

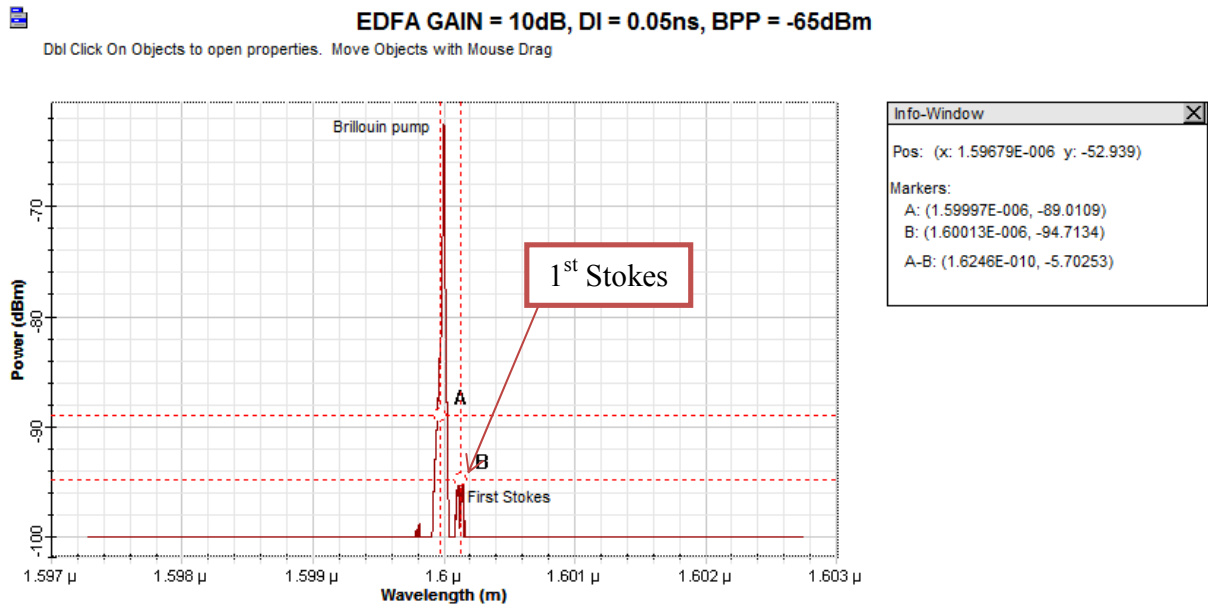


Figure 4.2: Output spectrum of lasing condition in the cavity at EDFA gain of 10dBm

Figure 4.3 shows the output power against the EDFA gain. 10dB is the threshold as it can be clearly seen in figure 4.3, once the threshold above, the BEFL output power increases in tandem with increase in EDFA gain. This illustration is depicted in figure 4.3

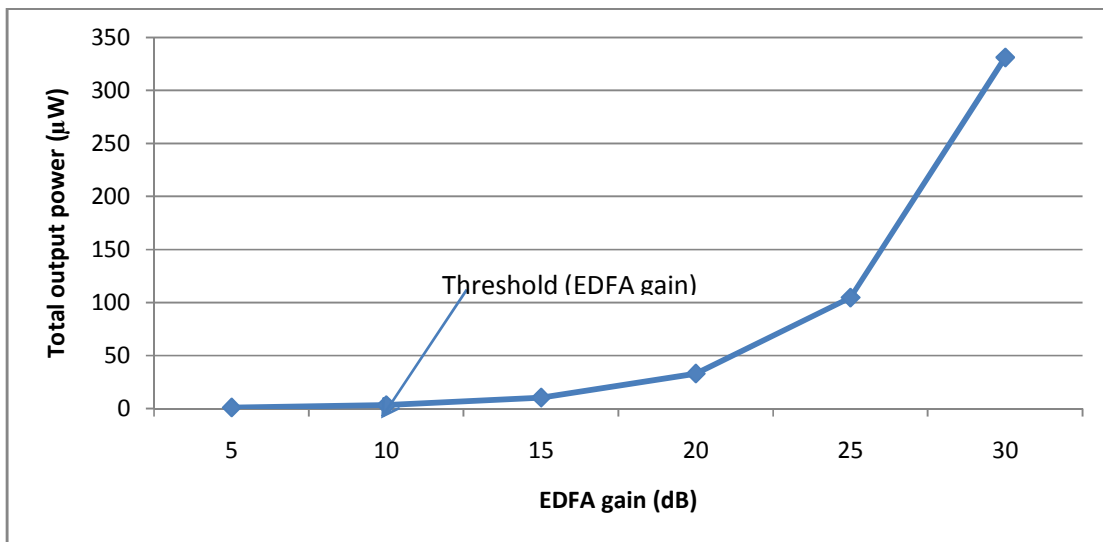


Figure 4.3: Output power of the BEFL against the EDF pump power.

The measured laser output power variation with respect to EDFA gain is illustrated in Figure 4.3. The EDFA gain is varied from 0 to 30dB to characterize the lasing behavior and to determine the lasing threshold. As shown in Figure 4.3, lasing characterized by a sudden increase in emission and is obtained when the EDFA gain level reaches 10dB at fixed BP power of -65dBm. The threshold should occur when the gain compensates for the cavity loss and after exceeding the threshold level the output increases almost linearly with the EDFA gain or pump power and more Stokes lines will be generated.

Threshold values can be obtained at different values of EDFA gain and Brillouin pump power. In view of this, there is need to observe the different threshold value of EDFA gain and the corresponding value of Brillouin gain needed to generate the first lasing line and keep the cavity in a lasing mode. The lasing characteristics of the system were then studied. Figure 4.4 shows the plot of the Brillouin pump power against the EDFA gain for the lasing threshold of the proposed system. The lasing threshold decays exponentially which agreed with theory. It can be seen from Figure 4.4 that higher EDFA gain requires small BP power and vice versa, for the first order stoke to be appeared.

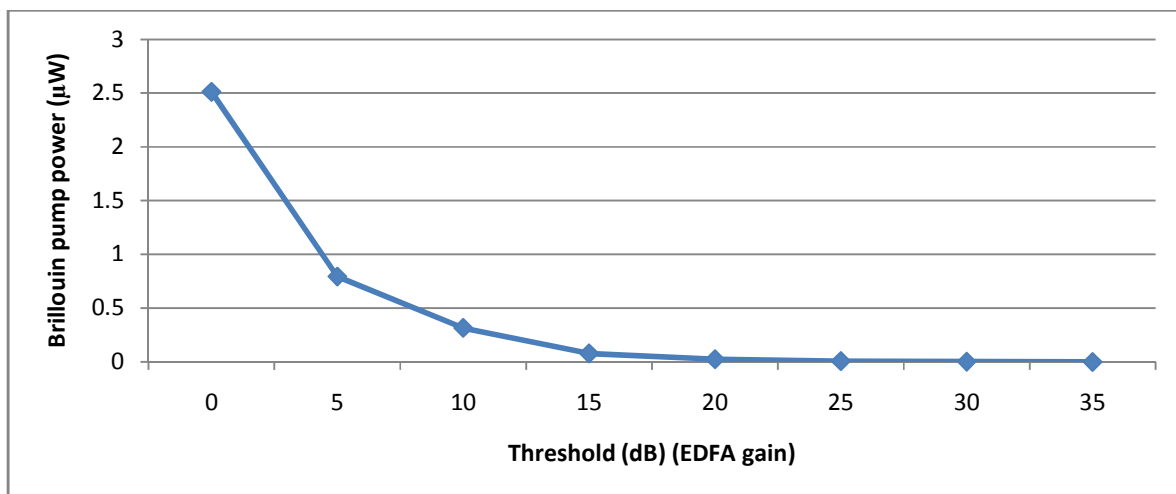


Figure 4.4: Lasing threshold of the delay Interferometer assisted MBEFL laser system.

For the second Stokes signal to appear, the first Stokes peak power needs to be saturated with gain because it will serve as Brillouin pump for the second Stokes signal and the second Stokes power will serve as BP power for the generation of the third Stokes and soon. In general the previous Stokes signal provides energy to generate next Stokes signal. So, there is need to increase the EDFA gain beyond the threshold level for the multiple wavelength generation. Therefore, threshold for others higher order Stokes need to be determined. The value of the EDFA gain that generates a specific order of Stokes signal is the threshold for that specific order of Stokes. Figure 4.5 clearly shows the increment of the Stokes signal threshold level with the Stokes order. Higher order Stokes signals have a higher threshold level because a high gain enables high oscillating energy in the cavity, which guarantees a higher Stokes signal power oscillating in the cavity.

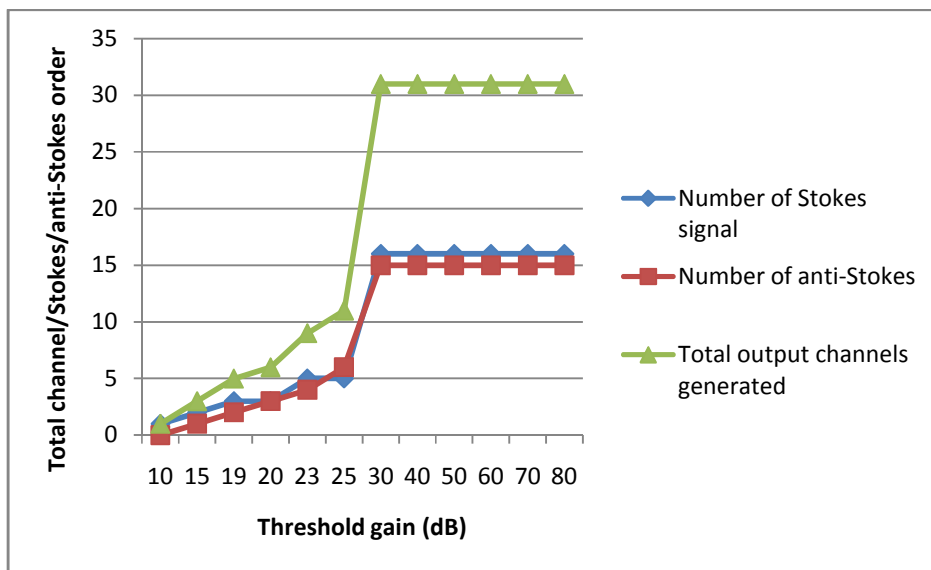


Figure 4.5: The Stokes and anti-Stokes (total output channels) signals lasing threshold as a Measure of EDFA gain

4.2.2 Effect of EDFA Gain on Channel (Stokes and anti-Stokes) Peak Power

In this study, the Brillouin pump power and wavelength are fixed at values of -65dBm and 1600nm respectively while the EDFA gain is vary between the ranges of 10dB to 80dB. Below 10dB of EDFA gain no Stokes or anti-Stokes signal were generated as shown in figure 4.1. At 10dB of EDFA gain and above, the peak power for each Brillouin Stokes and anti-Stokes signal increases with the increase in EDFA gain as shown in figure 4.6 and figure 4.7 respectively. This is due to the increase of gain in the cavity. Then, it is also observed that the power of the subsequent Stokes lines is typically lower than that of the previous Stokes line because each subsequent Stokes is generated with the energy of the previous Stokes, thus slightly reducing Stokes peak power as the conversion of Brillouin pump signal to Stokes signal is always less than unity i.e. the output power is always less than the injected power in the cavity due to photon depletion inside the cavity which result to loss of some energy injected. Anti-Stokes lines are obvious with the increase in Brillouin gain inside the cavity and these anti-Stokes signals are produced by four wave mixing. Therefore, at optimum EDFA gain of 80dB the Stokes peak power obtained between -23.67dBm and -46.92dBm respectively while the anti-Stokes peak power obtained between -28.38dBm and -47.51dBm respectively.

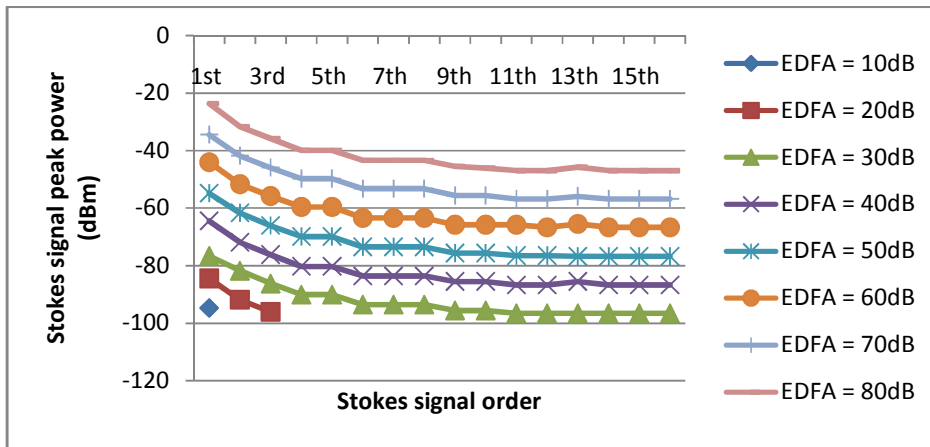


Figure 4.6: Stokes peak power plotted against Stokes signal order at different EDFA gain

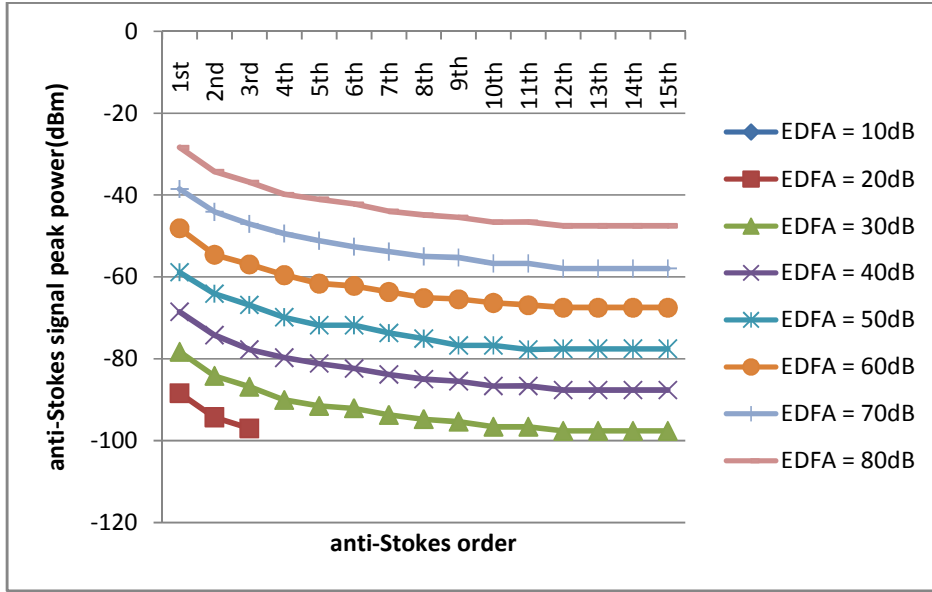


Figure 4.7: anti-Stokes peak power plotted against Stokes signal order at different EDFA gain

4.2.3 Effect of EDFA Gain on Number of Channels (Stokes and anti-Stokes Signal)

Figure 4.8 shows the number of Brillouin Stokes and anti-Stokes that are respectively generated by stimulated Brillouin scattering and four wave mixing with increase in EDFA gain. The numbers of lasing lines of Stokes and anti-Stokes signal increases as the EDFA gain increases. This is because of sufficient signal power for higher order Stokes signal to pump the SMF-fiber and causes the process of multiple generations of lasing lines to continue. As it is depicted in figure 4.8, at EDFA gain of 10dB, only one Stokes signal is produced. When the EDFA gain tuned at 30dB up till optimum EDFA gain of 80dB, maximum of 31-output channels of Stokes and anti-Stokes signals are maintained. However, further increase in EDFA gain beyond the optimum EDFA gain could not increase the lasing lines but lead to reduction in number of output channels (Stokes and anti-Stokes signals) as can be shown in spectrum of figure 4.9. This is attributed to the gain reduction in the cavity as a result of depletion of photon

inside the cavity, which reduces the erbium gain as the EDFA gain increases beyond the optimum value.

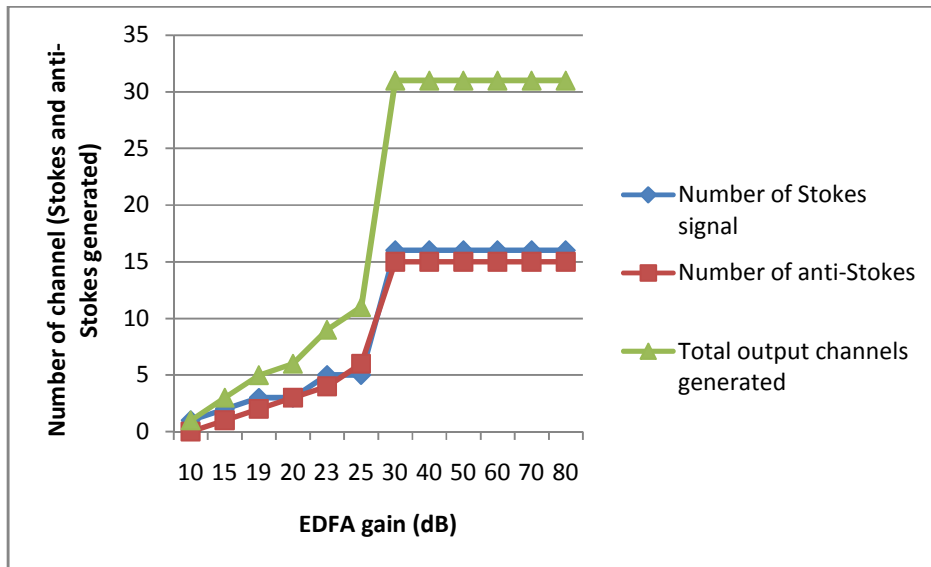


Figure 4.8: Number of Output channels (Stokes and anti-Stokes signals) generated against EDFA gain

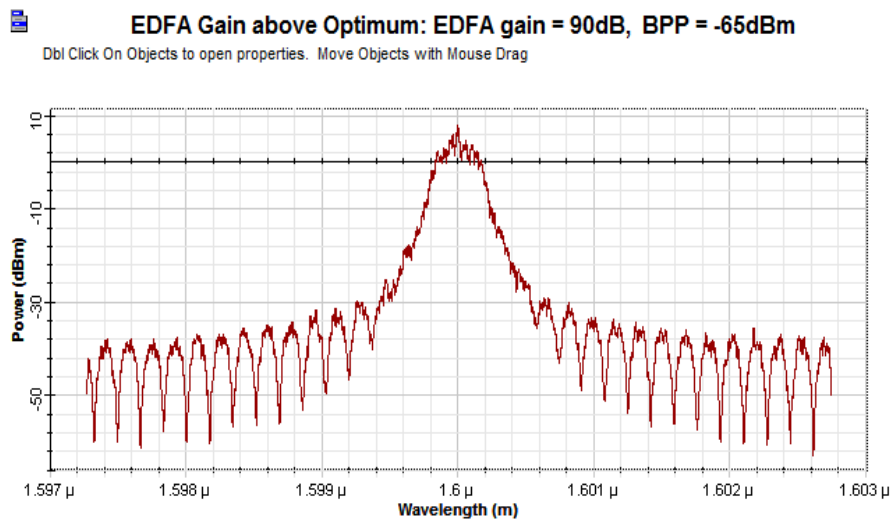


Figure 4.9: Wavelength spectrum of EDFA gain above optimum

4.3 Effect of Brillouin Pump Power

The effect of Brillouin pump power on the performance of this proposed multi-wavelength laser has been investigated at fixed EDFA gain of 10dB i.e. threshold value and the Brillouin wavelength of 1600nm then, the number of Stokes and anti-Stokes signal equivalent to the total output channel, channel peak powers and wavelength spacing are observed at various Brillouin pump power varying from -65dBm to 6dBm. Below -65dBm, the SBS gain is not sufficient enough to compensate for the loss inside the cavity as Brillouin generation in SMF-fiber requires a BP with sufficient power to reach the threshold, and line-width less than the Brillouin gain bandwidth for good efficiency. Hence, multi-wavelength generation cannot be performed in that case. Therefore, it should be noted that Brillouin optimum occurs at EDFA gain and Brillouin gain of 10dB and 6dBm respectively. At this optimum condition of the cavity, a maximum of thirty one (31) output channels of 16-Stokes and 15-anti-Stokes signals with wavelength spacing of 0.17nm as depicted in Figure 4.10.

OPTIMUM 31-CHANNELS WITH 0.17nm SPACING FOR EDFA GAIN =10dB, BPP = 6dBm, DI = 0.05nm
 Dbl Click On Objects to open properties. Move Objects with Mouse Drag

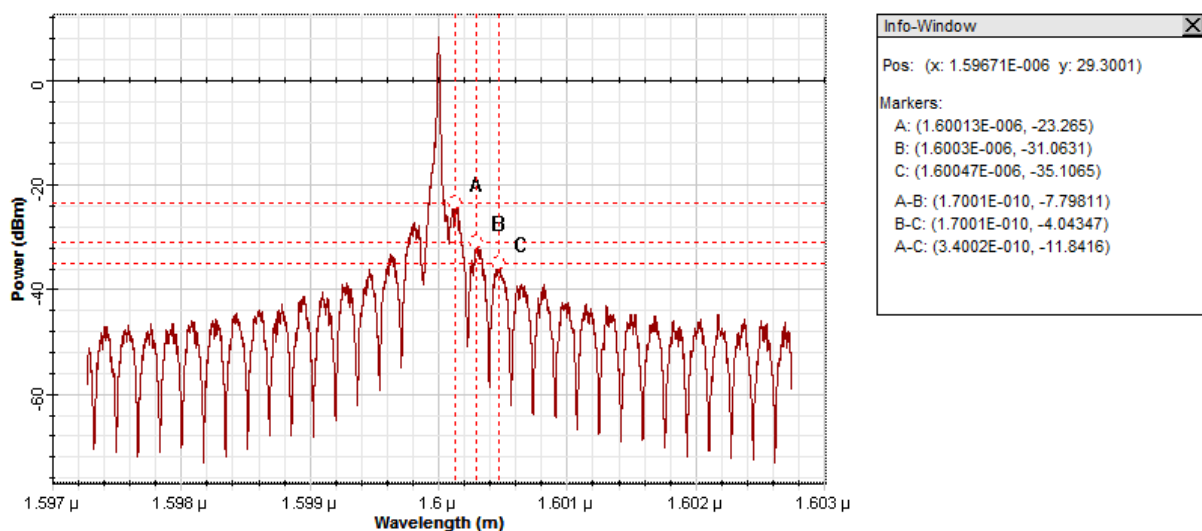


Figure 4.10: Thirty one output channels, 0.17nm (20GHz) spacing of Brillouin fiber laser comb.

At too much Brillouin pump power above the Brillouin optimum of 6dBm, the number of lasing lines is reduced due to the photon or pump depletion in the cavity and not providing enough gains for more channels to be generated, as can be seen in figure 4.11

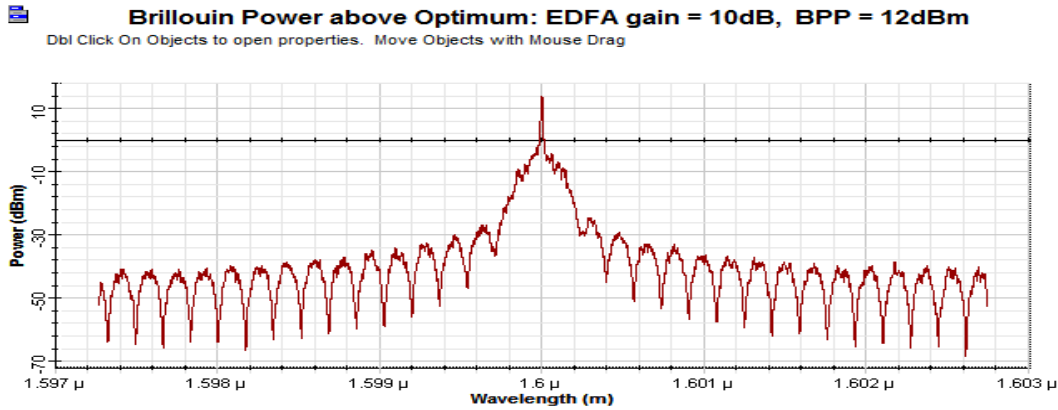


Figure 4.11: Wavelength spectrum of Brillouin power above optimum

4.3.1 Effect of Brillouin Pump power on Stokes and Anti-Stokes Peak Power

The higher Brillouin gain in the cavity provides sufficient signal power for higher order Stokes signals to pump the SMF and maintain cascading process of the multiple channels. From figure 4.10, the peak power of Stokes and anti-Stokes signal can be measured for different BP powers. Figure 4.12 shows the measured peak power for the Stokes and figure 4.13 for anti-Stokes at different Brillouin pump power. It was observed that, the peak power increases as the BP power increases due to high Brillouin gain in the cavity and that the peak power of each subsequent Stokes is generated with the energy of the previous Stokes due to the fact that, the input power conversion to Brillouin Stokes from Brillouin pump is always less than the actual input power injected because of reduction in Brillouin gain. At optimum BP power of 6dBm, the peak powers of the Stokes signals obtained between -23.26dBm and -46.08dBm respectively while the anti-Stokes signals peak powers obtained between -27.60dBm and -44.66dBm

respectively. The anti-Stokes signals are generated due to degenerate four wave mixing (FWM) effect which occurs between co-propagating Brillouin pump power and the photons in the cavity. In addition, anti-Stokes signals are obvious with high Brillouin pump power.

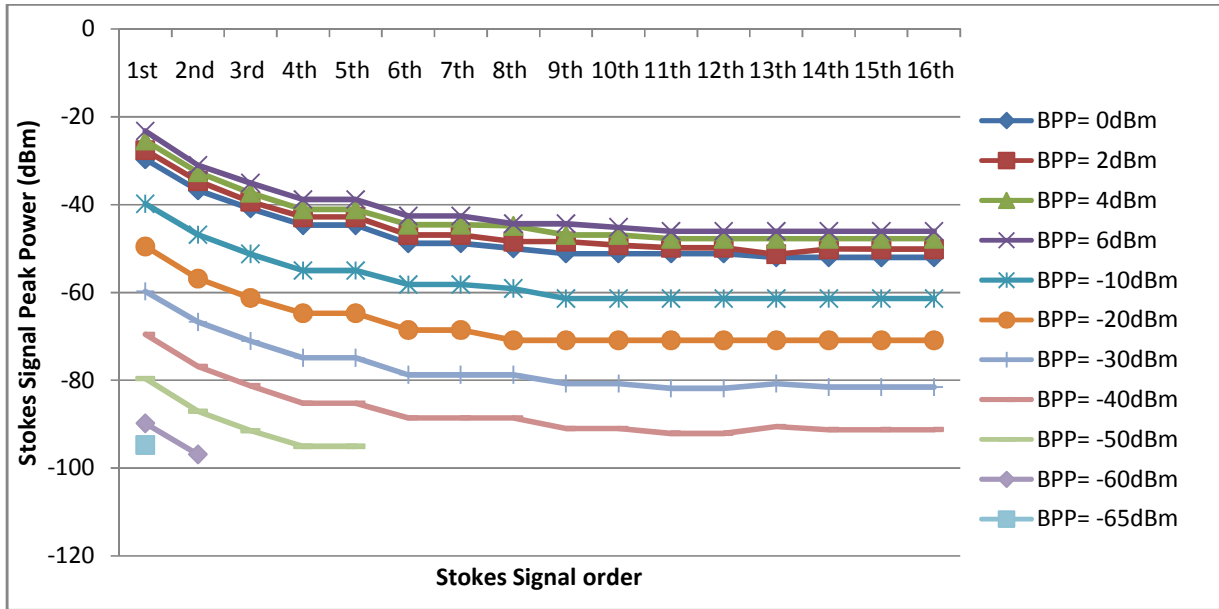


Figure 4.12: Stokes peak power plotted against Stokes signal order at different BP power

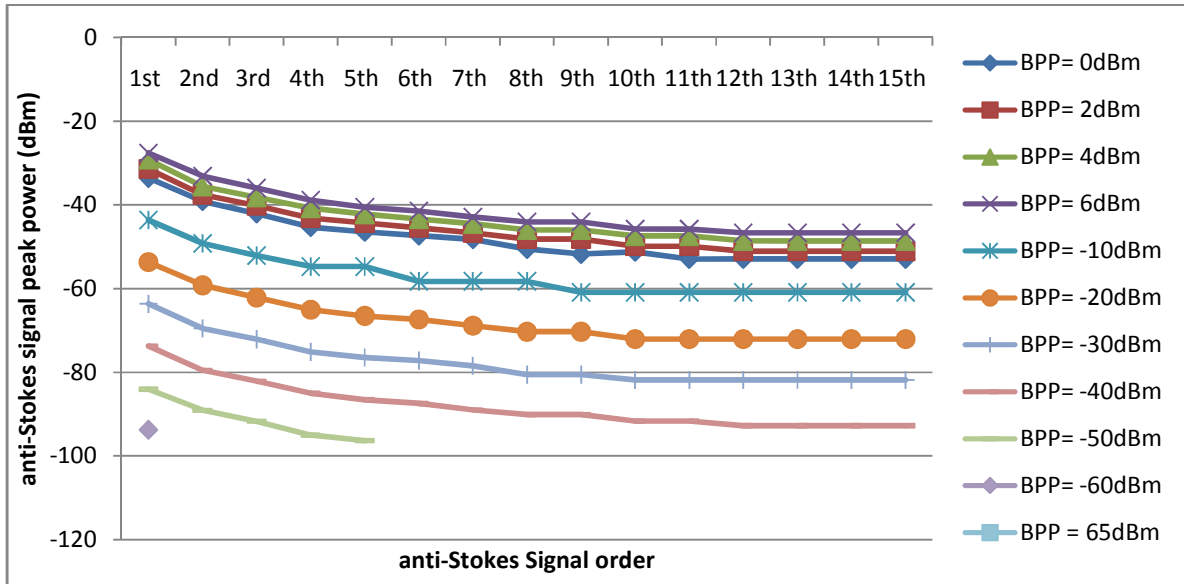


Figure 4.13: anti-Stokes peak power plotted against Stokes signal order at different BP power

4.3.2 Effect of Brillouin Pump Power on the Number of Channel (Stokes and Anti-Stokes Signal)

Figure 4.14 shows the relationship between the number of output channels generated and the Brillouin pump power. As it is depicted in figure 4.14, it is noticed that, as BP power increases from -65dBm to -40dBm, the number of output channel increases. This is attributed to the increase in nonlinear Brillouin gain as the BP power increases. From -40dBm to 6dBm the cavity become saturated with 31-output channels of Stokes and anti-Stokes signals. Increase the BP power above 6dBm leads to decrease in number of output channel generated. The reason being that, at BP power above 6dBm, extremely high BP power is injected into the cavity and too big Brillouin pump power injected depletes the photons in the cavity, which causes the higher order Stokes not to have enough gain to lase. The higher order Stokes or anti-Stokes then demanded large power to seed an additional channel (Stokes or anti-Stokes) inside the cavity and the total number of the channels reduced as can be shown by the spectrum of figure 4.14

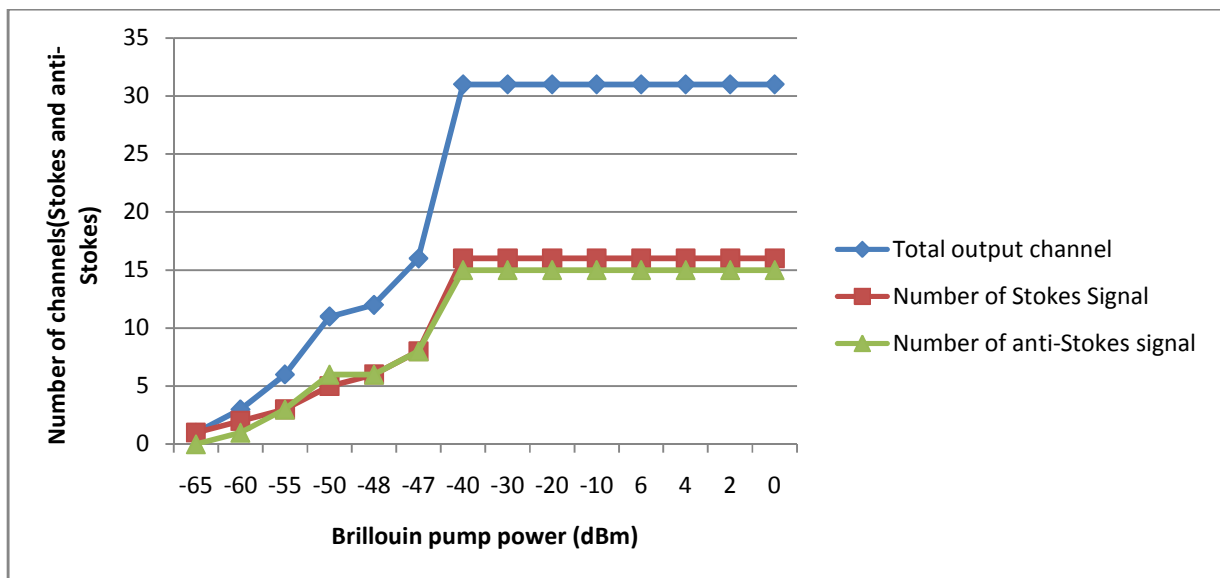


Figure 4.14: Number of Output channels (Stokes and anti-Stokes signals) generated against BP power

4.4 Effect of Brillouin Pump Wavelength

The impact of Brillouin wavelength on the performance of multi-wavelength laser, most especially, the number of output channels generated and the total output power determine the laser tunability. Therefore, the tunability measured refers to as tuning range and is defined here as the range of Brillouin pump wavelengths which produce the Stokes and anti-Stokes signals without restriction from self lasing cavity mode. The self lasing is eliminated by high Brillouin gain inside the cavity. In this study the effect of Brillouin wavelength on number of channel and the total output power is investigated. The simulation is carried out by varying the Brillouin wavelength over the entire L-band region of 1565nm to 1625nm at optimum condition of the cavity at fixed EDFA gain, time delay of interferometer, Brillouin pump power of 10dB, 0.05ns and 6dBm respectively.

4.4.1 Effect of Brillouin Wavelength on Number of Output Channels and Total output Channel

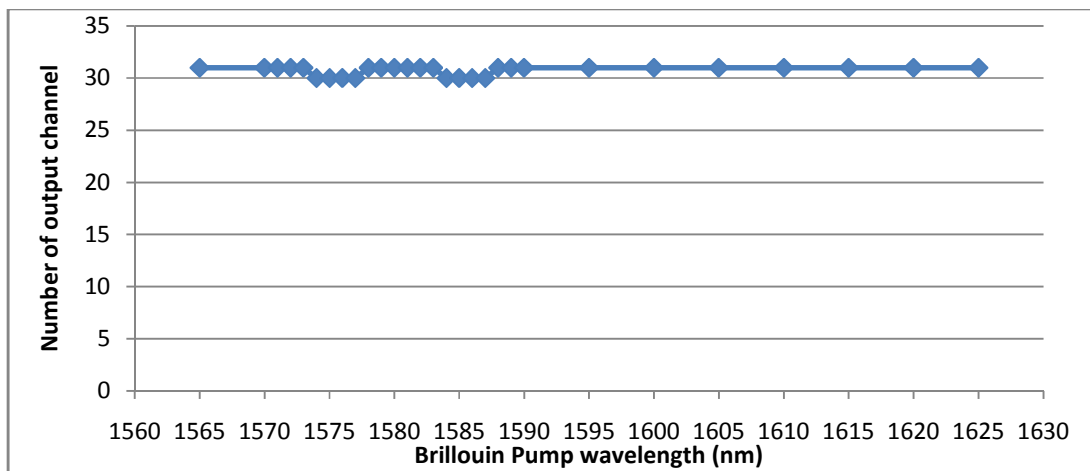


Figure 4.15: Number of output channels generated against BP wavelengths

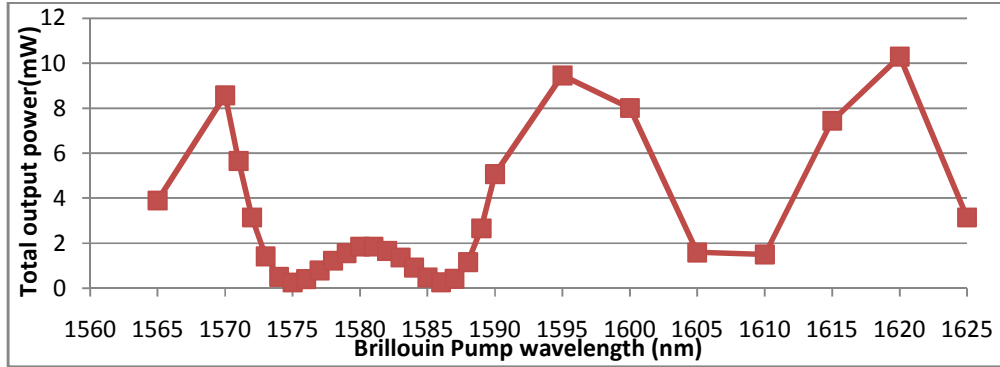


Figure 4.16: Total output power against BP wavelengths

From figure 4.15, it is observed that 31 output channels are generated at BP wavelength range of 1588nm to 1625nm, 1565nm to 1573nm and 1578nm to 1583nm respectively, also BP wavelength range of 1574nm to 1577nm and 1584nm to 1587nm generated about 30 output channels as depicted in figure 4.15. Figure 4.16 shows the relationship between the total Brillouin wavelength and the total output power. It is observed that the highest power of 10.30mW is obtained at 1620nm BP wavelength with 31 output channels. Generally, the maximum output power is obtained at Brillouin wavelength with 31 output channels. Also the output power of 30 output channels is lower as compare to the 31 output channels. This is due to the fact that, the total output power of the laser system depends on the number of channels generated. Meanwhile, the higher the total output power, the higher the number of output channels generated. The output spectra of the Brillouin wavelength tuned over the entire L-Band of 1565nm to 1625nm at step of 5nm corresponding to time delay, EDFA gain and BPP at 0.05ns, 10dB and 6dBm is clearly shown in appendix A. In the output spectra, it is observed that 31 channels of Stokes and anti-Stokes signals were generated at Brillouin wavelength range of 1588nm to 1625nm (37nm bandwidth) of L-band with double Brillouin shift equivalent to wavelength channel spacing of 0.17nm.

Therefore, the broad wavelength tuning of 37nm with 31-output channels was obtained by properly compensate for the loss in the cavity by high Brillouin pump power and erbium-doped fiber amplifier. Also the broad tuning range allows a robust operation of the BEFL as the BP does not need to be accurately wavelength matched, provided that it generates sufficient Brillouin gain.

4.5 Effect of Time Delay

In this study, the channel spacing as well as the number of output channels of the transmitted wave produced by L-Band MBEFL utilizing delay interferometer filter has been observed and analyzed. The time delay of Interferometer delay filter varies from 0.01ns to 0.1ns.

4.5.1 Effect of Interferometer Time Delay on Channel Spacing

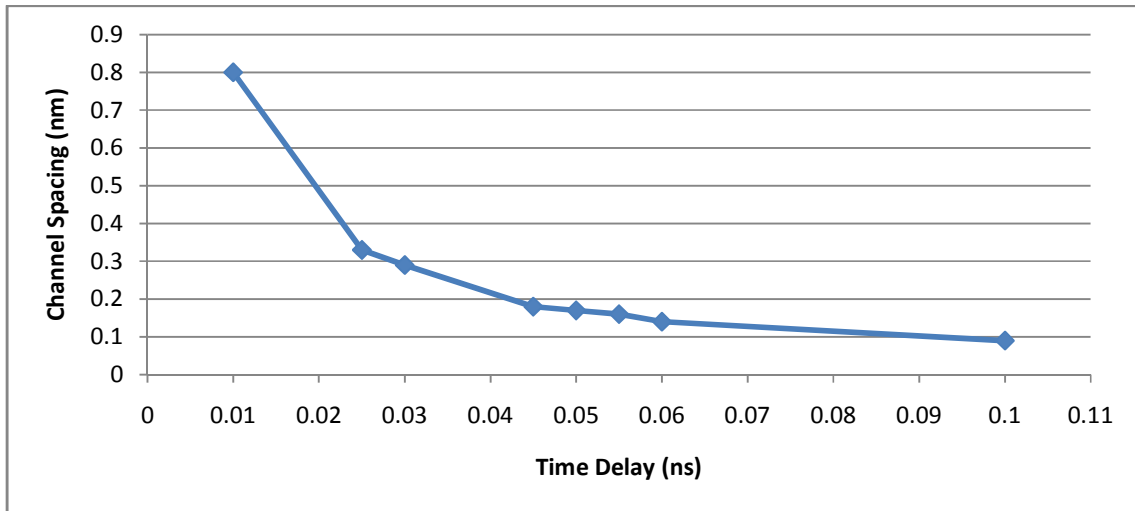


Figure 4.17: Wavelength channel spacing against Time delay of the Delay Interferometer.

Figure 4.17 compares the wavelength spacing between two adjacent transmission peaks at different Time delay of Delay Interferometer. At 0.025ns, wavelength spacing between two adjacent transmission peaks is 0.33nm while the adjacent wavelength spacing between two transmission peaks is 0.17nm at 0.05ns of time delay of Interferometer delay filter. The reason

being that the delay Interferometer acts as a comb filter which makes the wavelengths that match the peaks of the comb oscillates when it is in laser cavity. The wavelength spacing between two adjacent transmission peaks is 0.33nm ($t=0.025\text{ns}$) for one transmission trip. For the double transmission trip which is equivalent to two cascaded delay interferometer, channel spacing between two adjacent transmission peaks is reduced. Therefore multiple transmission trips through delay interferometer will further reduce the wavelength spacing and increase the number of output channels. The variation of time delay of Delay Interferometer filter with the Channel spacing produced is depicted in Figure 4.17.

4.5.2 Effect of Interferometer Time Delay on Number of Output Channels Generated

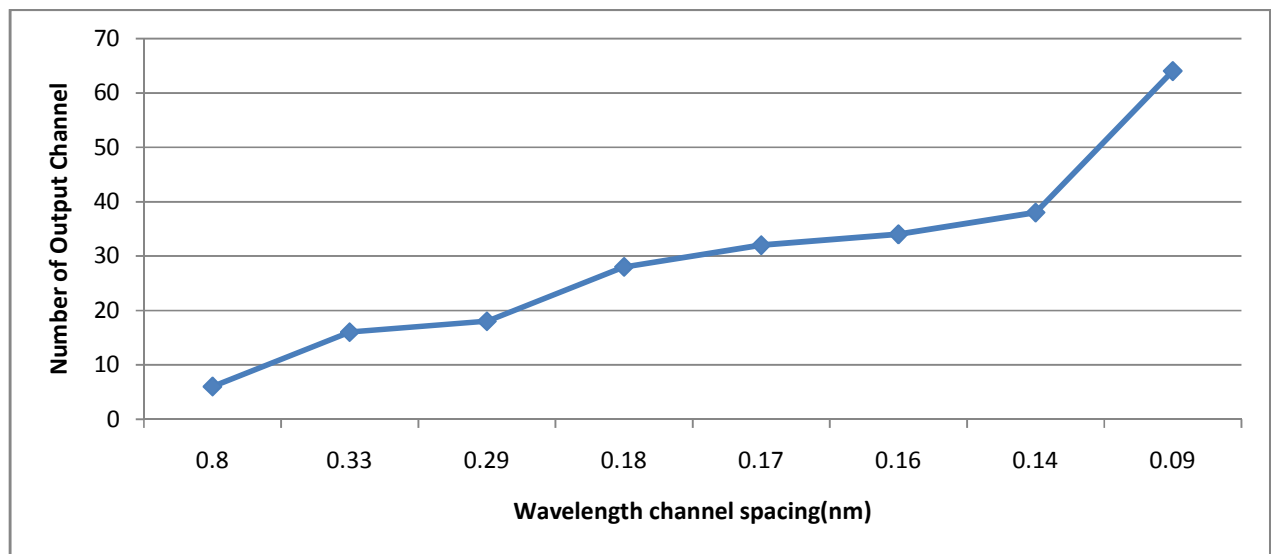


Figure 4.18: Output Channels generated against wavelength channel spacing.

Figure 4.18 compares the number of output channels generated at different channel spacing determined by time delay Interferometer. It is clearly shown that 64 output channels of both Stokes and Anti-Stokes Signals are generated with channel spacing of 0.08nm generated at Time delay of 0.01ns while at 0.33nm channel spacing generated at time delay of 0.025ns only

15 output channels is produced. The least output channels of six are produced at time delay interferometer of 0.01ns with wavelength spacing of 0.8nm. The variation of output channels with channel spacing corresponding to time delay is shown in figure 4.18.

In order to check the wavelength channel spacing and the number of output channel generated, the fine spectra of time delay range of 0.01nm to 0.1nm at EDFA gain, Brillouin wavelength and power of 10dB, 1600nm and 6dBm are shown in Appendix B

4.6 Optical Signal to Noise Ratio (OSNR) Analysis

OSNR analysis is performed by comparing the peak power of the generated channels with the highest noise level. The noise power and channel peak power in this study are measured by DWDM analyzer and Optical spectrum analyzer respectively. This study is performed at Brillouin pump power of 6dBm at different EDFA gain of 0dB and 10dB.

Figure 4.19 depicts the OSNR of the output channels in corresponding with the optimum condition of the laser cavity with parameters of time delay, EDFA gain and Brillouin pump power and wavelength set at 0.05ns, 10dB, 6dBm and 1600nm respectively. The OSNR of the first to sixteen channels of the Stokes of the transmitted signal are obtained between 30.03dBm and 7.21dBm while OSNR for anti-Stokes signal were obtained between 25.69dBm and 6.63dBm respectively. This implies that the channels with high peak power possess good OSNR; this is due to the fact that, the channel with low peak power is seriously affected by noise in the medium. Therefore, the higher the peak power, the better the OSNR. This is illustrated in the figure 4.19.

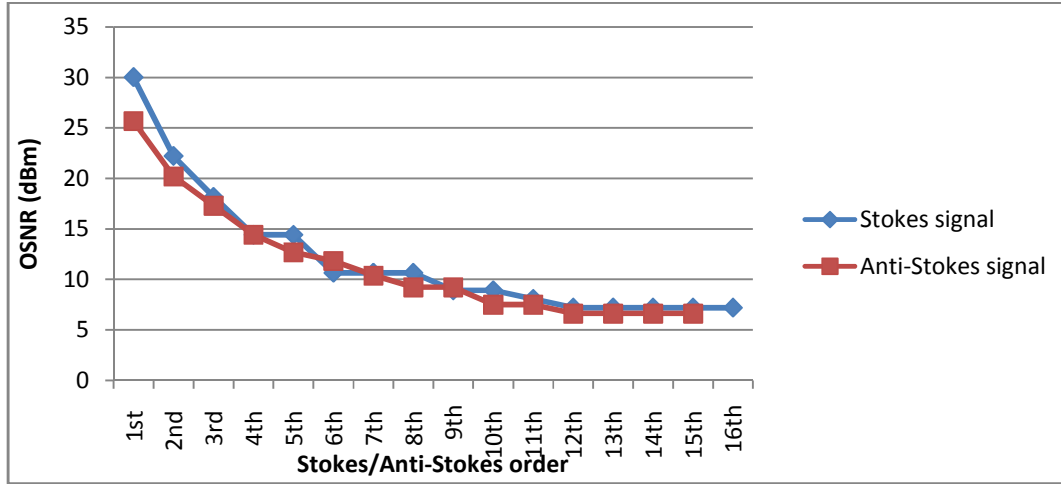


Figure 4.19: Output Channels (Stokes and anti-Stokes signal) OSNR corresponding to EDFA Gain and Brillouin power of 10dB and 6dBm.

4.6.1 Effect of Brillouin Pump Power on OSNR.

Figure 4.20 and figure 4.21 show the relationship between the OSNR and order of Stokes/anti-Stokes at different Brillouin pump power. It was observed that increase in BP power leads to increase in OSNR. This is because the ASE noise has been suppressed by the high Brillouin pump power which as a result yields a better achievement in OSNR quality. The first channel of Stokes and anti-Stokes were obtained at 23.59dBm and 19.76dBm for (BP power of 0dBm) which increases to 25.66dBm and 21.86dBm at (BP power of 2dBm) and also increases to 27.89dBm and 24.12dBm at (BP power of 4dBm), then the maximum OSNR is obtained at optimum condition of the laser cavity mode having OSNR of 30.03dBm and 25.69dBm at (BP power of 6dBm) for the first channel of Stokes and anti-Stokes signal.

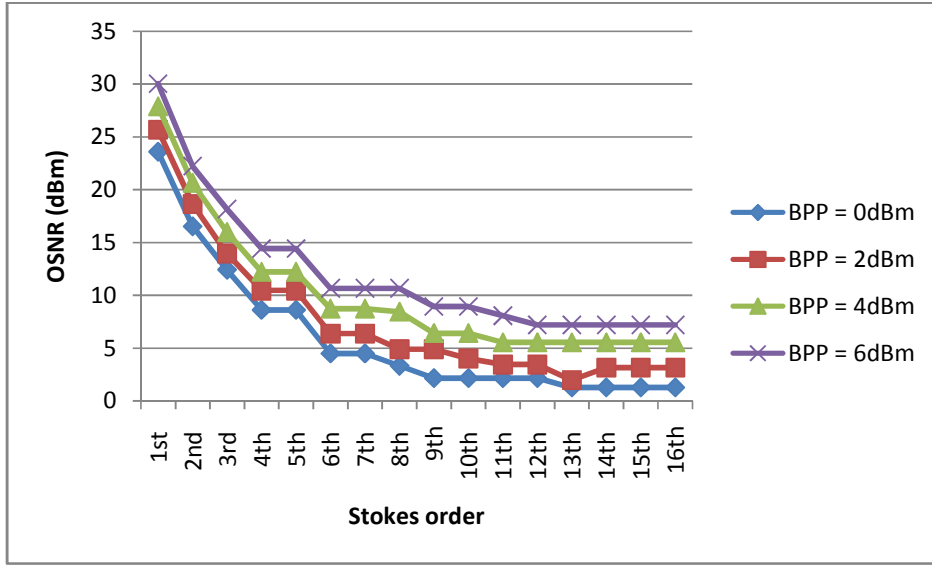


Figure 4.20: Stokes signal OSNR at different Brillouin pump power.

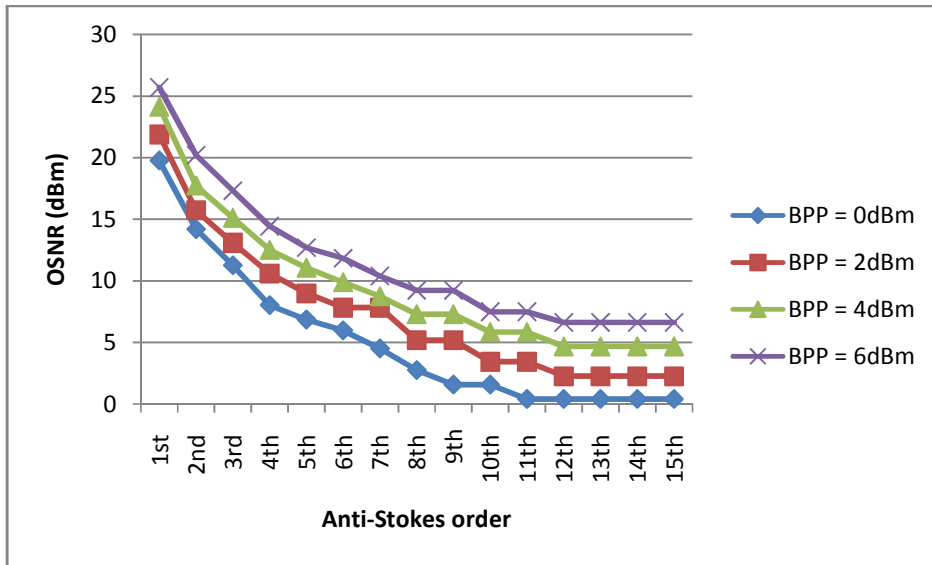


Figure 4.21: Anti-Stokes signal OSNR at different Brillouin pump power.

4.6.2 Effect of EDFA on OSNR

Figure 4.22 and figure 4.23 depict OSNR of the generated output channels of Stokes and anti-Stokes signal at different EDFA gain. It is observed that as EDFA gain increases, the OSNR is decreasing. At 0dB of EDFA gain, the OSNR were obtained between 9.03dBm and 31.92dBm

for Stokes channel and anti-Stokes OSNR obtained between 8.47dBm and 27.82dBm, while at 10dB of EDFA gain, Stokes OSNR obtained between 7.21dBm and 30.03dBm, then anti-Stokes OSNR generated between the range of 6.63dBm and 25.69dBm of minimum to maximum values. The reason being that, at high EDFA gain, amplified spontaneous emission (ASE) noise generated through EDF amplifier is predominantly in the channel which suppress the Brillouin gain and drastically reduce the OSNR of the output channels as can be illustrated in Figure 4.22 and figure 4.23. Therefore, at low EDFA gain, BP power is almost enough to suppress the ASE from the amplifier to provide a better OSNR while at higher ASE due to increase in EDFA gain, BP power is unable to compete with the laser cavity modes which causes reduction in the OSNR quality.

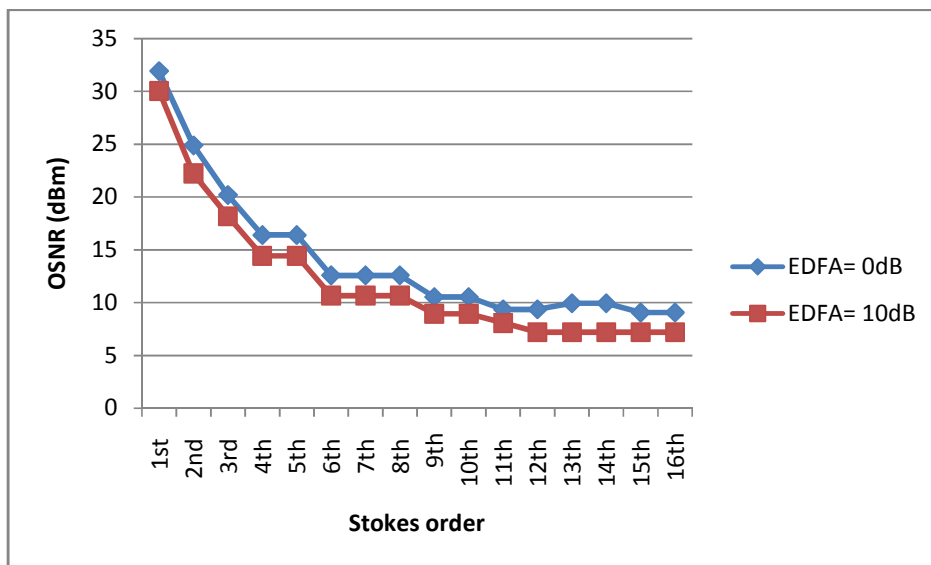


Figure 4.22: Stokes signal OSNR at different EDFA gain.

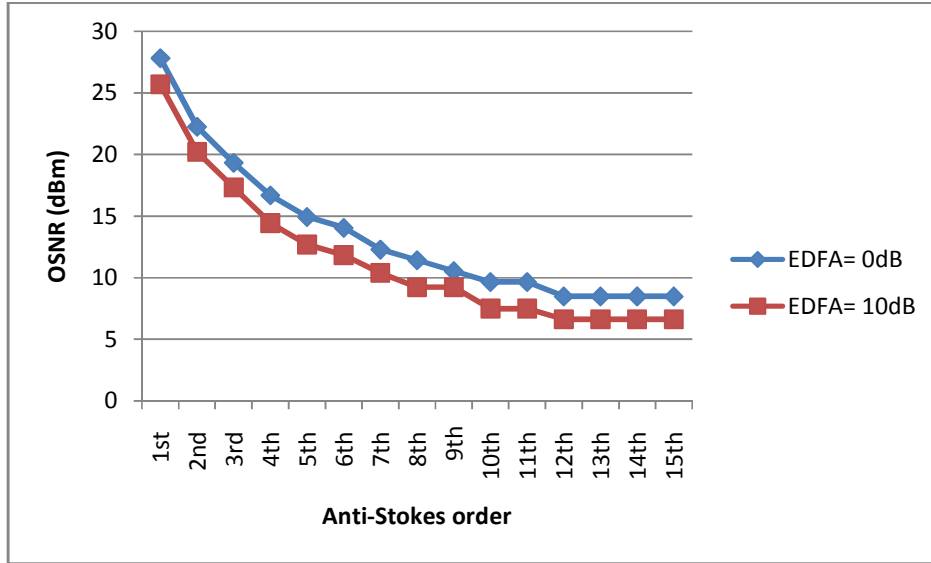


Figure 4.23: Anti-Stokes signal OSNR at different EDFA gain.

4.7 Major Contribution

Majority of the MWBEFL designs generates fixed and narrow spacing in order of 10GHz (0.08nm) between adjacent channels which cause difficulty in channels multiplexing and limit the practical contributions of the MWBEFL. Also, many scenarios have been studied and the finding was that, most MWBEFL either generate large number of output channels with low tuning range and vice versa. In view of this, controlled spaced MWBEFL is designed in simulation environment of optisystem optical simulation software with the following contributions:

(1) Variation in channel spacing between adjacent channels which can be clearly seen in figure 4.17 and figure 4.18, the spectra of which are shown as in Appendix B. Up to 0.8nm (93.75GHz) spacing between adjacent channels was able to obtain and this can make the channel de-multiplexing process easier as compared to de-multiplexing at narrow spacing of 10 or 20GHz.

(2) The maximum of 31-channel was obtained at 0.16nm (20GHz) which can be tuned at 37nm, also, when the spacing was adjusted to 0.08nm (10GHz) maximum of 64-channel was obtained which makes this MWBEFL suitable to be used in DWDM system.

CHAPTER FIVE

SUMMARY, CONCLUSION AND RECOMMENDATIONS

5.1 Summary

This chapter has presented simulation results and thorough analysis of the characteristics of a BEFL system. Simulation results are extensively used in discussing the effects of EDFA gain, Brillouin pump power, Brillouin pump wavelength and time delay on the performance parameters of the BEFL system. Threshold of 10dB EDFA gain was obtained at 1600 nm with -65dBm launched Brillouin pump power. The lasing characteristics curve also evident that, a higher Brillouin power will requires small EDFA gain (threshold) and vice versa. Multi-wavelength generation also obtained at EDFA gain higher than threshold. Thirty-one (31) output channels with wavelength spacing of 0.16nm were generated with the value of EDFA gain from 30dB to 80dB. Above 80dB, the number of lasing lines (output channels) reduced due to pump depletion that suppresses the gain in the cavity.

The peak power of the channels (Stokes and Anti-Stokes) in relation with the EDFA gain and Brillouin pump power has been verified. The peak power increases with increase in both EDFA gain and Brillouin pump power up to the optimum condition of the cavity.

Wavelength channel spacing analysis has been done. The time delay of delay interferometer is a channel spacing determinant in this research and it has direct relationship with the number of output channels generated but inversely related with wavelength channel spacing i.e. increase in time delay lead to increase in number of output channel generated but decrease in wavelength channel spacing. The least and highest time delay of 0.01 and 0.1ns produced channel spacing of 0.8 and 0.09nm with six (6) and sixty-four (64) output channels respectively.

Brillouin wavelength tuning has been properly analyzed, the tuning is performed within the L-band region and the obtainable thirty-one (31) output channels can be tuned within the bandwidth of 37nm of 1588 – 1625nm range of L-band. This broadband range is attributed to the high gain of EDFA and Brillouin that compensate for the loss in the cavity and avoid the self lasing mode in the cavity.

Finally, OSNR analysis is performed by comparing the peak power of the individual channels with the highest level of noise in the channel. OSNR values obtainable at optimum Brillouin power (6dBm) while fixed the EDFA gain at 10dB are 30.03dBm and 25.69dBm for the first channel of Stokes and anti-Stokes signal respectively. It is also deduced that the OSNR increases with increase in Brillouin gain but decrease with increase in EDFA gain due to amplified spontaneous emission that contribute to the higher level of noise in the channel.

5.2 Conclusion

The L-band multi-wavelength Brillouin erbium fiber laser with adjustable channel spacing has been proposed. The design utilized amplifier (EDFA) and CW laser as Brillouin pump for multi-wavelength operation. The comb filter called delay interferometer is used for channel spacing adjustment. Optisystem optical simulation software is used to simulate this MWBEFL. The simulation was carried out using various design parameters including, EDFA gain, Brillouin pump power, Brillouin pump wavelength and time delay.

The effect of design parameters on performance parameters of threshold power, peak power of the Stokes and anti-Stokes signal, number of channels generated, tuning range and OSNR has been observed. The Threshold of this MBEFL is obtained at 10dB with first Stokes appeared at peak power of -94.71dBm above. Optimum EDFA gain is 80dBm and 31 output

channels with 20GHz spacing of 16 Stokes signal appeared with peak power ranged from -23.67dBm to -46.92dBm and about 15 anti-Stokes signal obtained which range from -28.38dBm to -47.51dBm. All these 31 channels can be tuned within the L-band range of 1588nm to 1625nm of about 37nm bandwidth. Also, the maximum channel spacing obtainable between adjacent channels is 0.8nm (93.75GHz) and only 6 channels were able to produce at time delay of 0.01ns while about 64 channels with 0.08nm (10GHz) spacing were generated at time delay of 0.1ns.

OSNR measures the bit error rate (BER) of the system. OSNR performance obtained to be better at optimum Brillouin pump power of 6dBm while kept EDFA gain at threshold value of 10dB. Therefore, the measured OSNR for the first and sixteenth of Stokes signals obtained at 30.03dBm and 7.21dBm while measured OSNR for the first and fifteenth anti-Stokes signals are obtained at 25.69dBm and 6.63dBm respectively. More so, channels with high peak power possess good OSNR; this is due to the fact that, the channel with low peak power is seriously affected by noise in the medium. Therefore, the higher the peak power, the better the OSNR. In general, at high BP power, the amplified spontaneous emission (ASE) generated from EDFA is almost suppressed to provide a better achievement of OSNR. However, the BP power is unable to compete with laser cavity modes at higher ASE from EDFA which reduces the quality of OSNR. Therefore this study has been able to achieve a great performance of high number of output channel with broad tuning range and good OSNR. High peak power of the channels with adjustable wavelength channel spacing has also been achieved.

5.3 Recommendation for Future Works

At the moment, the aim of this research is to develop an L-Band multi-wavelength Brillouin fiber laser with adjustable spacing between adjacent channels. Although this research

target has been fulfilled, but there are some limitations encountered along the way. These limitations and suggested solutions includes

1. Difficulty in generating the channels peak power at the same amplitude. There may be improvement on this by including filter in the MWBEFL structure with proper arrangement of other fiber components.
2. Inability of the MWBEFL to produce more than 6 output channels at spacing of 0.8nm (93.7GHz). Possibly by mirroring the cavity, so that both transmitted and reflected signal are measured as a single output, there may be increase in number of lasing lines and tuning range.
3. Inability to observe variation in peak power of the channel over some period of time. Further study should focus on this because it determines the system stability.

REFERENCES

- Alasia1 D., Fernandez A., Abrardi L., Brichard B. and Thevenaz L., (2006) “The effects of gamma-radiation on the properties of Brillouin scattering in standard Ge-doped optical fibres,” *Meas. Sci. Technol.* Vol.17, PP. 1091–1094.
- Ali N.M, Anyi C. L., Arof H.and Harun S. W., (2013) “*Brillouin erbium fiber laser generation in a figure-of-eight configuration with double Brillouin frequency spacing*” IEEE Int. Conf. Proc. Electronics, Communications and Photonics Conf. (SIECPC) Saudi International PP 1–4
- Al-Mansoori M.H and Malin P, (2009) “*Novel multiwavelength L-Band BEFL utilizing double pass Brillouin pump preamplified technique*”, IEEE Quantum Electron., Vol. 15, no. 2, PP 415–421.
- Al-Mansoori M.H and Mahdi M.A, (2011) “*Broadly tunable L-Band multi-wavelength BEFL utilizing nonlinear amplified loop mirror filter*”, Optics Exp., Vol. 19, PP 23981–23988.
- Bellemare A., KarásekM., Rochette M., LaRochelle S., and Têtu M., (2000) “*Room temperature multifrequency erbium-doped fiber lasers anchored on the ITU frequencygrid*,” J. Lightwave Technol. Vol.18 no. 6, PP 825–831.
- Boyd, R. W., (1992) “Nonlinear Optics”, Academic Press, San Diego, CA.
- Boyd R. W, (2007) “Nonlinear Optics,” Third edition, Academic Press, San Diego, CA.
- Buttner T F S, Kabakova I V, Hudson D D, Pant R, Li E and Eggelton B J (2012) “*Multi-wavelength gratings formed via cascaded stimulated Brillouin scattering*” Opt. Express 20 26434–440
- Chen Z., Ma S. and Dutta N.K. (2009) “*Multi-wavelength fiber ring laser based on a semiconductor and fiber gain medium*” OPTICS EXPRESS, Vol. 17, No. 3 2
- Cowle, G.J., and Stepanov, D.Y. (1996). *Hybrid Brillouin/Erbium fiber laser*. Optics Letter, Vol. 21, PP 1250-1252.
- Das G. and Chaboyer Z.J, (2009) “*Single-wavelength fiber laser with 250 mW output power at 1.57 μ m*,” Optics Express, vol. 17, no. 10, PP. 7750-7755.
- Desurvire E.,(2002) “*Erbium-Doped Fiber Amplifiers, Principles and Application*”, Wiley Interscience
- Dichie R.H., (1958) “*Molecular amplification and generation systems and methods*,” U. S. Patent Vol. 2 PP. 851 652.

Haddud T. A, Al-Mansoori M. H, Zamzuri A. K, Shaharudin S, Abdullah M. K and Mahdi M. A, (2005) "24-Line of Brillouin-Erbium fiber Laser utilizing a Fabry-Perot cavity in L-band", microwave and Opt. Technol. Lett., Vol. 45, No. 2, PP. 165-167.

Han K, Xu XJ and Liu ZJ (2012) Chin. Phys. B Vol. 21 PP 054-205

Harun S.W, Tamchek N., Poopalan P. and Ahmed H., (2002), "*Efficient multi-wavelength generation of Brillouin/erbium fiber laser at 1600-nm region*", Microwave Opt. Technol. Lett. Vol. 35, PP 506–508.

Ippen E.P and Stolen R.H, (1972) "Stimulated Brillouin scattering in optical fibers," Appl. Phys. Lett., Vol. 21, PP. 539-540.

Jackson J.D, (1962) Classical Electrodynamics, first ed., John Wiley & Sons, Inc., New York.

Kamaljit Singh Bhatia, Kaler R. S., Kamal T.S., and Kaur, H., (2010). "*Simulative Analysis of operating conditions for Flat amplitude Multi-wavelength Brillouin-Raman comb fiber laser*," IJCST Vol.1 no. 1 PP. 89-92.

Karásek M. and Bellemare A, (2000), "*Numerical analysis of multi-frequency erbium-doped fiber ring laser employing periodic filter and frequency shifter*," IEE Proc. Optoelectron., Vol. 147, PP. 115–119.

Kasprowicz D., Drozdowski M., Majchrowski A., Michalski E., (2007) "Spectroscopic properties of KGd(WO₄)₂: (Er, Yb) single crystals studied by Brillouin scattering method," Optical Materials, Vol. 30, PP. 152–154.

Loayssa A., Benito D., and Garde M.J, (2000) "Optical carrier-suppression technique with a Brillouin-Erbium fiber laser," Opt. Lett., Vol. 25, PP. 197-199.

Mahdi M.A, Al-Mansoori M.H and Malin P., (2007) "*Enhancement of multi-wavelength generation in L-Band using a novel BEFL with a passive EDF booster section*" Optics Exp., Vol. 15, no. 18, PP. 11570-11575

Maiman T. H., (1960) "*Stimulated optical radiation in ruby masers*," Nature Vol. 187, pp. 493-494.

Matsukawa M., Shintani K., Tomohiro S. and Ohtori N., (2006) "Application of Brillouin scattering to the local anisotropy and birefringence measurements of thin layers," Ultrasonic Journal, Vol. 44, No. 22, PP. 1555-1559.

Mihelich F., Bacquet D., Zemmouri J., and Szriftgiser P., (2010) “*Ultra-high resolution spectral analysis based on a Brillouin fiber laser*”, Opt. Lett., Vol. 35, no. 3, PP. 432–434.

Mishra S.K., Tripathi S.N., Choudhary V., and Gupta B.D., (2014) “*SPR based fiber optic ammonia gas sensor utilizing nano-composite film of PMMA/reduced graphene oxide prepared by in situ polymerization*,” Sensor. Actuat. B-Chem, Vol. 199, PP 190–200

Min, B., Kim P., and Park, N. (2001). “*Flat amplitude equal spacing 798-channel Rayleigh assisted Brillouin/Raman multiwavelength comb generation in dispersion compensating fiber*,” IEEE Photonics Technology Letters, Vol. 13 no. 12 PP. 1352–1354.

Norcia S., Tonda-Goldstein S., Dolfi D., and Huignard J. P., (2003) “*Efficient single-mode Brillouin fiber laser for low-noise optical carrier reduction of microwave signals*,” Opt. Lett. Vol. 28, PP. 1888–1890.

Palais, J.C. (1998). *Fiber Optic Communications* (3rd edition). Prentice Hall, PP56.

Parvizi R., Arof H., Ali N.M., Ahmad H., and Harun S.W., (2011) “*0.16 nm spaced multi-wavelength Brillouin fiber laser in a figure-of-eight configuration*”, Opt. Laser Technol., Vol. 43, no. 4, PP 866–869, Jun. 2011.

Prokhorov A.M., (1958) “*Molecular amplifier and generator for sub millimeter waves*,” JETP (USSR), Vol. 34, PP. 1658–1659, June 1958; Sov. Phys. JETP, vol. 7, pp. 1140–1141, December 1958.

Ruffin A. B., (2004) “*Stimulated Brillouin Scattering: An overview of measurements, system impairments, and applications*,” NIST Symposium on Optical Fiber Measurements PP. 23–28.

Sandercock J., (1975) “*Some recent applications of Brillouin scattering in solid state*,” Advances in Solid State Physics, Switzerland, Vol. 15, PP.183–202.

Schawlow A.L and Townes C.H., (1958) “*Infrared and optical masers*,” Phys. Rev., Vol. 29, PP. 1940–1949

Shee Y G, Al-Mansoori M H, Ismail A, Hitam S and Mahdi M A (2011) “*Multi-wavelength Brillouin-erbium fiber laser with double-Brillouin-frequency spacing*” Opt. Express 19 1699–706

Siegman, A.E. (1986). *Lasers*. Mill Valley, CA, University Science Books, 474.

Shirazi M R, Harun S W, Biglary M and Ahmad H (2008) “*Linear cavity Brillouin fiber laser with improved characteristics*” Opt. Lett. 33 770–2

Shirazi M R and Biglary M (2012) “*Optical frequency comb generation using a new compacted hybrid Raman Bi-based erbium doped fiber amplifier in a linear cavity*” J. Opt. 14 125701

Shirazi M R, Harun S W and Ahmad H (2014) “*Multi-wavelength Brillouin Raman erbium-doped fiber laser generation in a linear cavity*” J. Opt. 16 035203

Shirazi M R, Mohamed Taib J, Dimyati K, Harun S W and Ahmad H (2013) “*Multi-wavelength Brillouin-Raman fiber laser generation assisted by multiple four-wave mixing processes in a ring cavity Laser*” Phys. 23 075108

Smith S.P, Zarinetchi F, and Ezekiel S, (1991). “*Narrow-line-width stimulated Brillouin fiber laser and applications,*” Opt. Lett. Vol. 16, PP 393–395.

Stepanov D.Y and Cowle G.J, (1997a) “*Multiple wavelength generation with Brillouin Erbium Fiber Laser*”, IEEE. Photon. Technol. Lett., Vol.8 PP

Stepanov D.Y and Cowle G.J, (1997b) “*Properties Brillouin/Erbium Fiber Laser*”, IEEE Quantum Electron., vol. 3 no 4, PP. 1049-1057

Stolen R.J., (1979) “*Polarization effects in Raman and Brillouin lasers,*” IEEE J. Quantum Electron., Vol.15, 1157–1160.

Taiwo A, Taiwo S, Sahbudin R.K.Z, Yaacob M.H, and Mokhtar M, (2014). “*Fiber sensor multiplexing techniques for quasi-distributed sensing,*” Opt. Laser Technol., Vol. 64, PP 34–40.

Tang J, Sun J, Zhao L, Chen T, Huang T and Zhoul Y (2011) “*Tunable multi-wavelength generation based on Brillouin erbium comb fiber laser assisted by multiple four-wave mixing processes*” Opt. Express 19 14682–9

Zamzuri, A.K., Mahdi, M. A., Al-Mansoori M. H., Samsuri N. Md., Ahmad A., and Islam M. S (2009), “*OSNR variation of multiple laser lines in Brillouin-Raman fiber laser,*” Opt. Express Vol. 17 no. 19 PP. 16904-16910.

Zarinetchi F, Smith S.P, and Ezekiel S, (1991) “*Stimulated Brillouin fiber optic laser gyroscope,*” Opt. Lett., Vol. 16, PP. 229–231.

Zhao Y, and Jackson S.D, (2005) “*Highly efficient free running cascaded Raman fiber laser that uses broadband pumping,*” Opt. Express Vol.13 no.12, PP 4731–4736

Appendix A

Output Spectra of the Brillouin Wavelength tuning

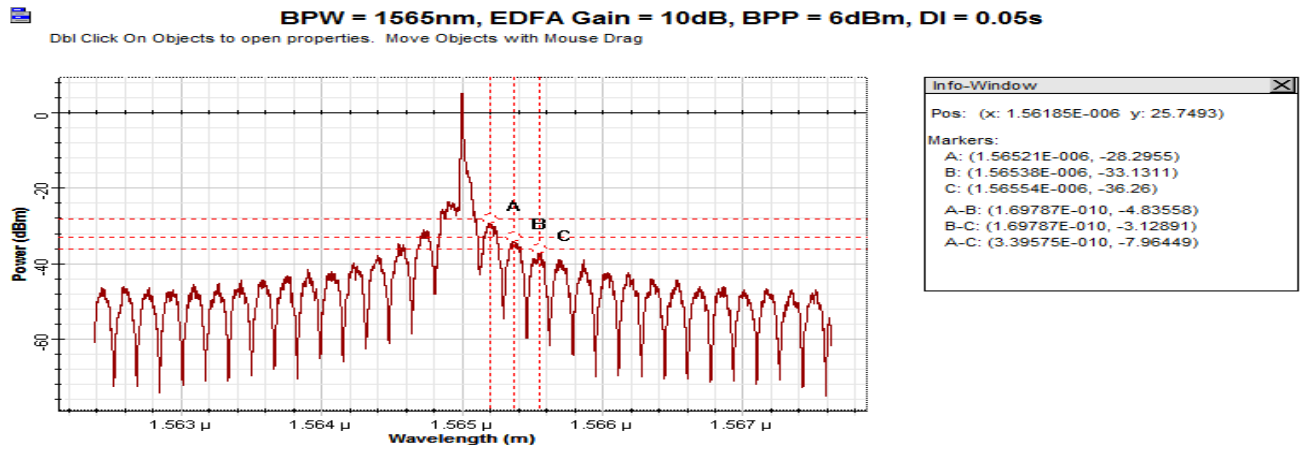


Figure A.1: Output spectra at Brillouin wavelength of 1565nm

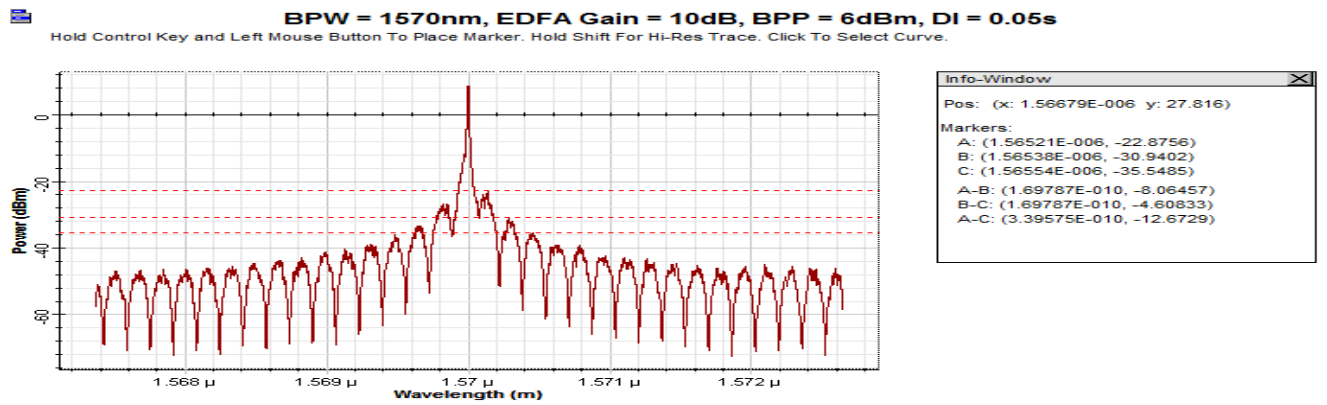


Figure A.2: Output spectra at Brillouin wavelength of 1570nm

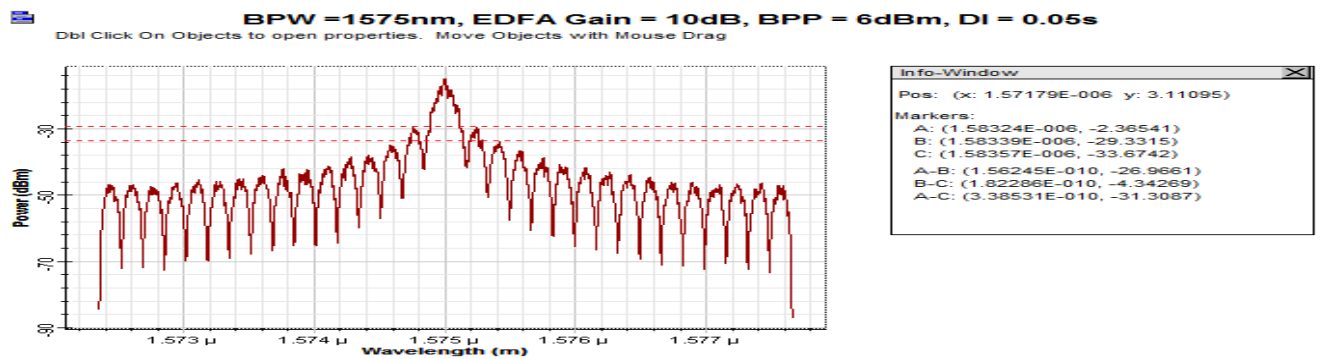


Figure A.3: Output spectra at Brillouin wavelength of 1575nm

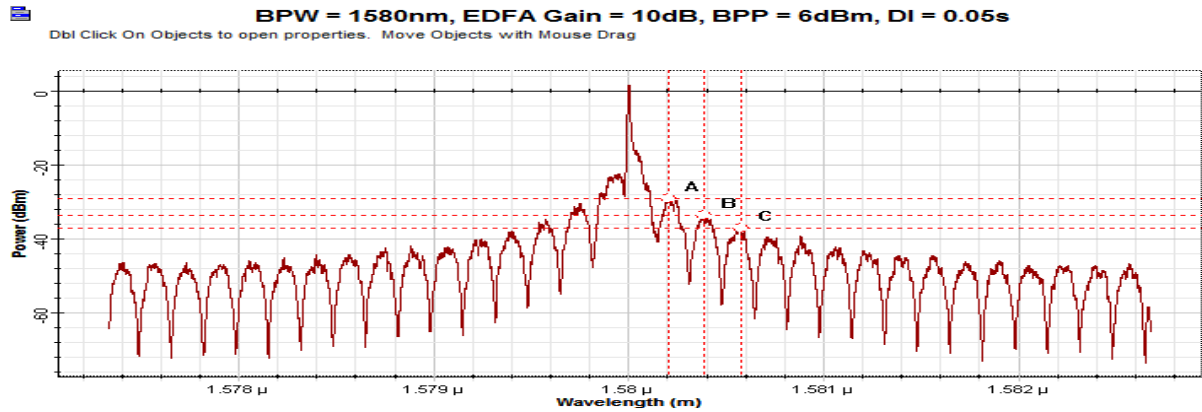


Figure A.4: Output spectra at Brillouin wavelength of 1580nm

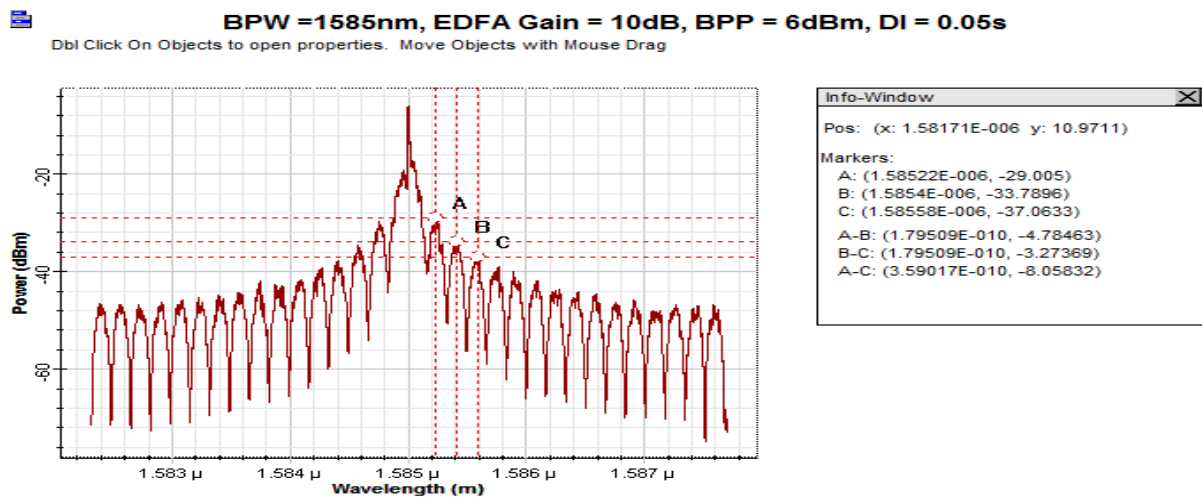


Figure A.5: Output spectra at Brillouin wavelength of 1585nm

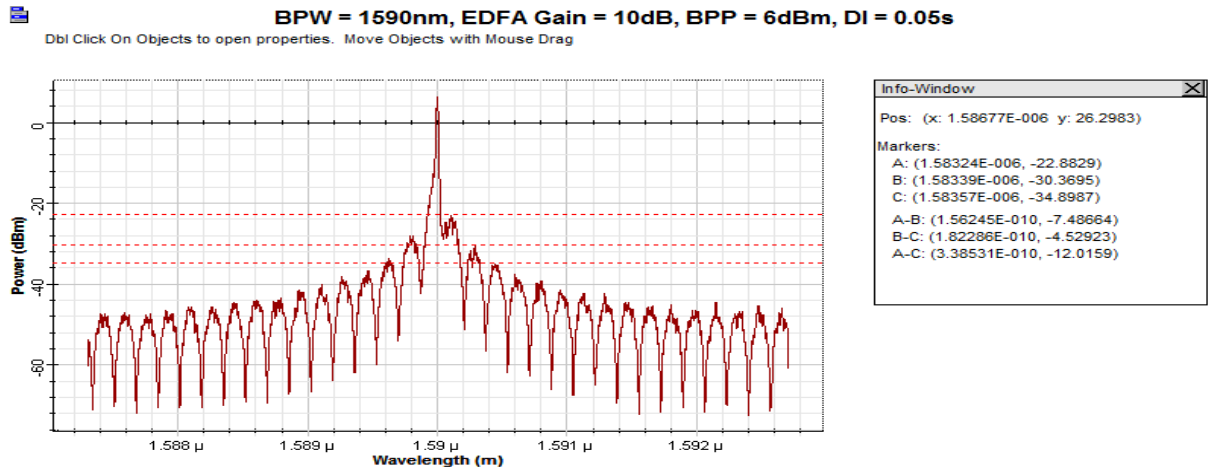


Figure A.6: Output spectra at Brillouin wavelength of 1590nm

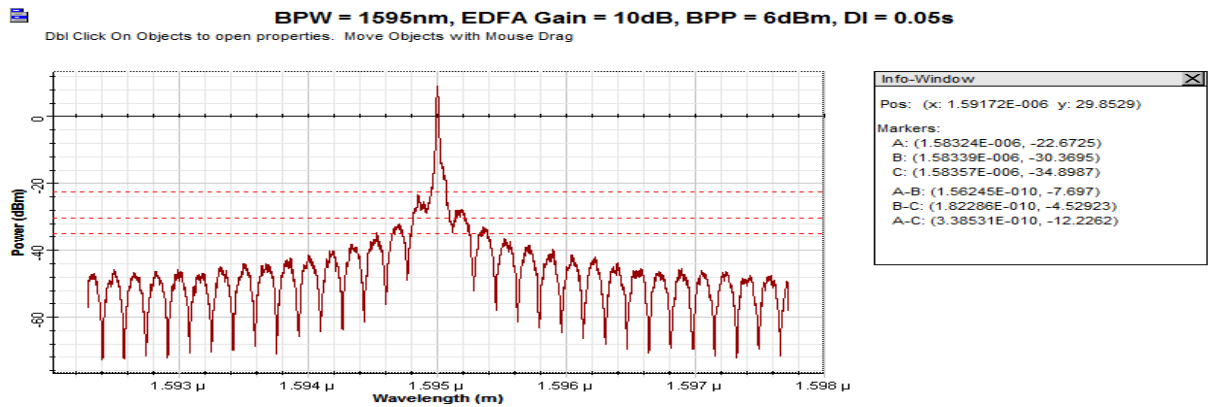


Figure A.7: Output spectra at Brillouin wavelength of 1595nm

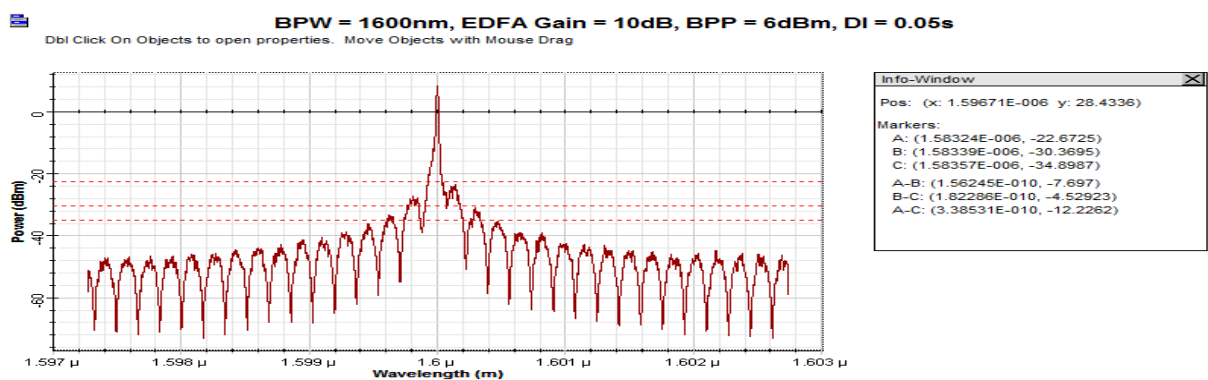


Figure A.8: Output spectra at Brillouin wavelength of 1600nm

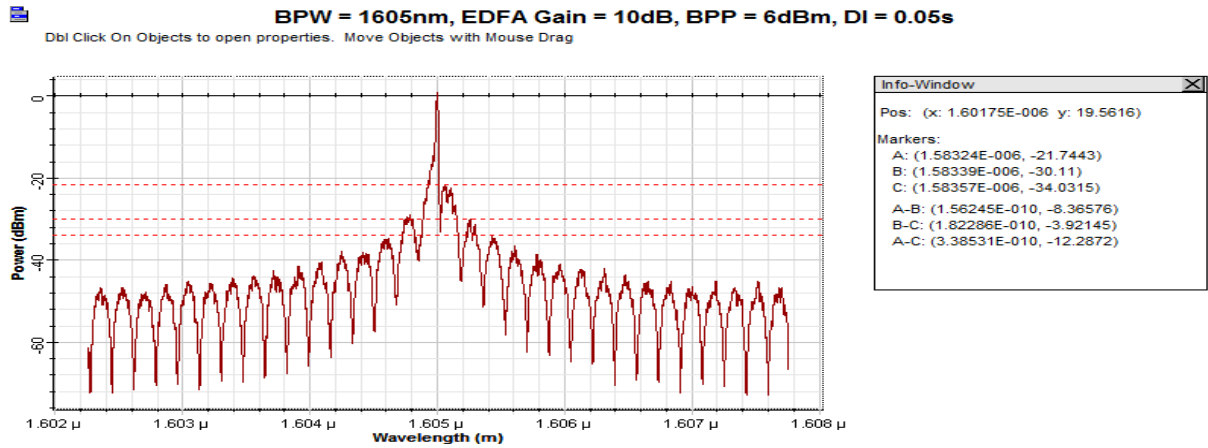


Figure A.9: Output spectra at Brillouin wavelength of 1605nm

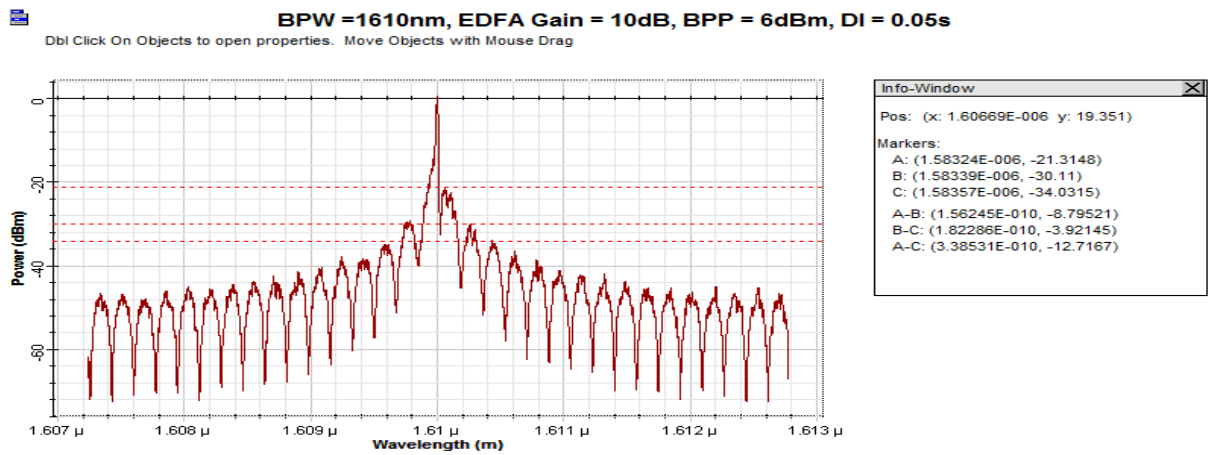


Figure A.10: Output spectra at Brillouin wavelength of 1565nm

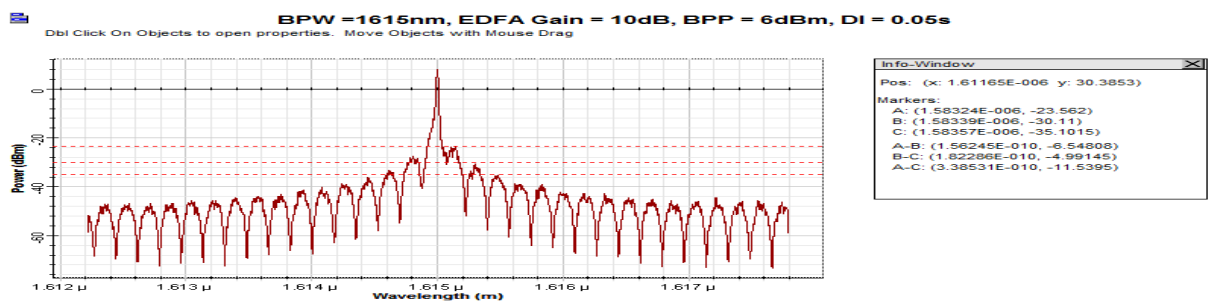


Figure A.11: Output spectra at Brillouin wavelength of 1615nm

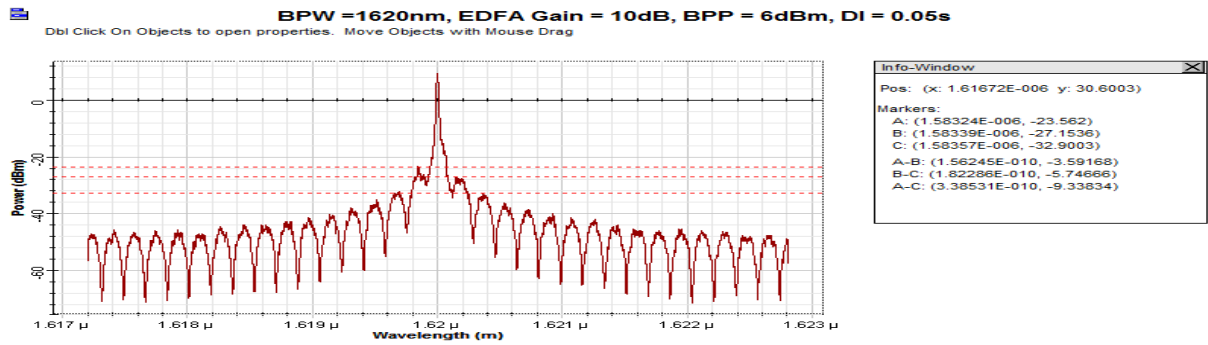


Figure A.12: Output spectra at Brillouin wavelength of 1620nm

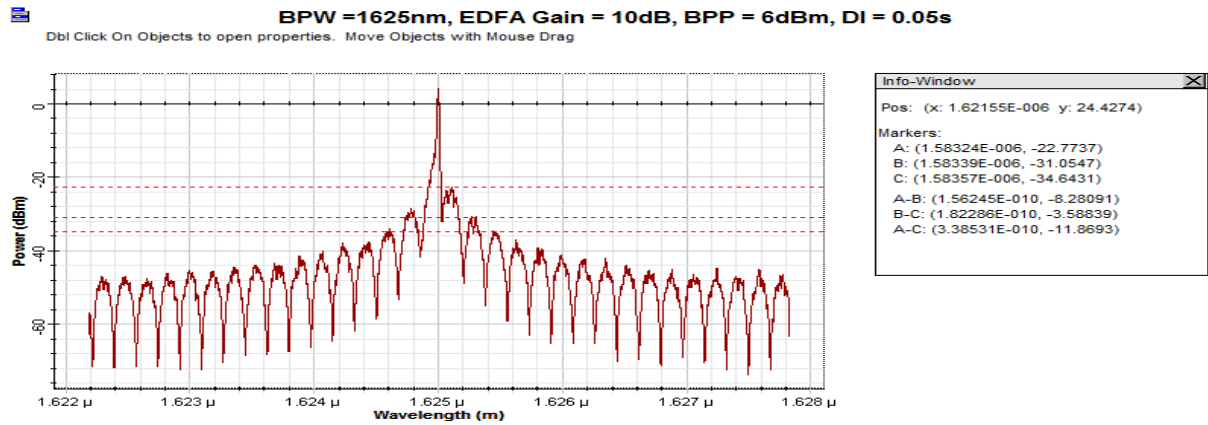


Figure A.13: Output spectra at Brillouin wavelength of 1625nm

Appendix B

Output Spectra of the Variation of time delay for channel spacing analysis

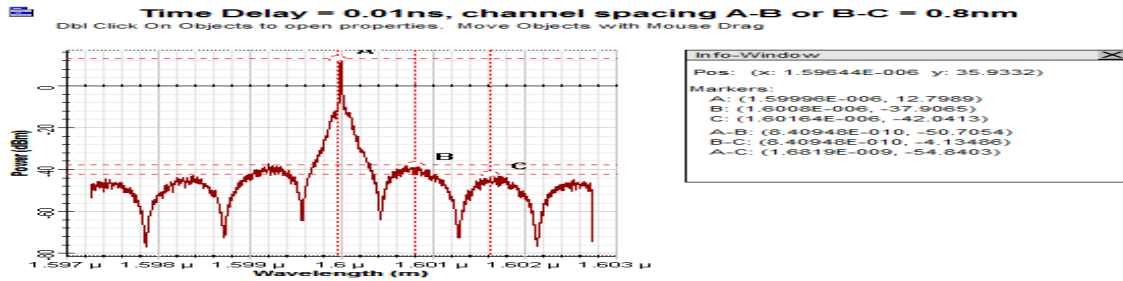


Figure B.1: Output spectra of wavelength Channel spacing and number of output channel generated at time delay of 0.01ns

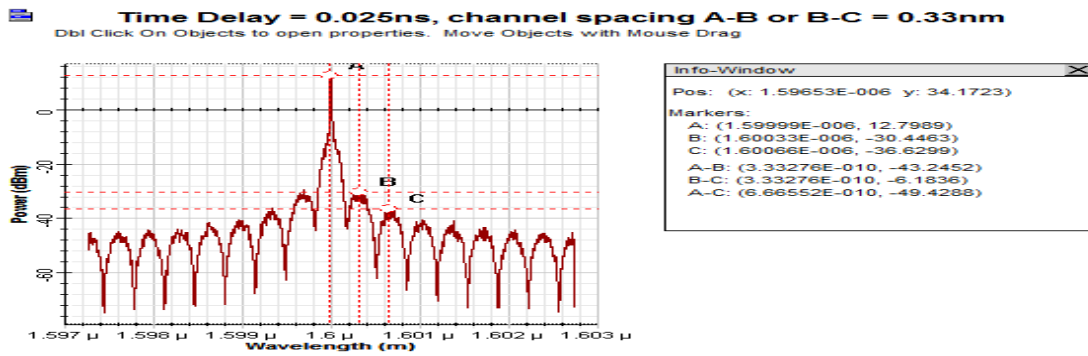


Figure B.2: Output spectra of wavelength Channel spacing and number of output channel generated at time delay of 0.025ns

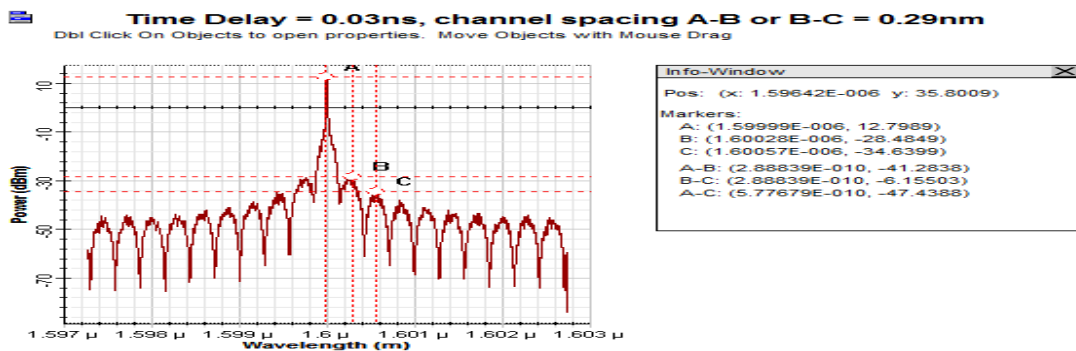


Figure B.3: Output spectra of wavelength Channel spacing and number of output channel generated at time delay of 0.03ns

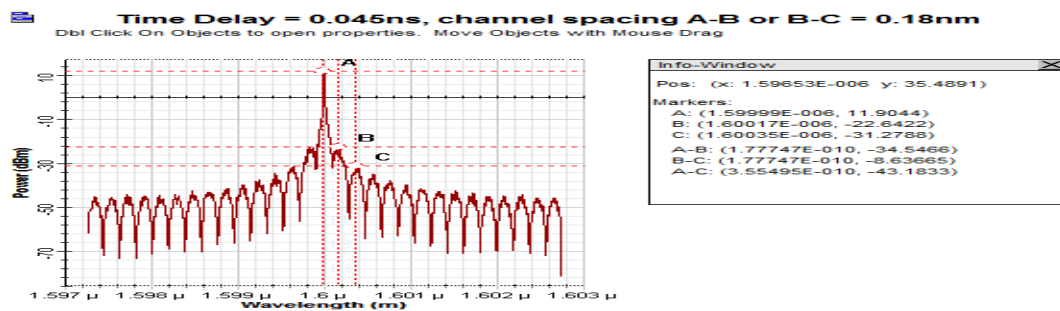


Figure B.4: Output spectra of wavelength Channel spacing and number of output channel generated at time delay of 0.045ns

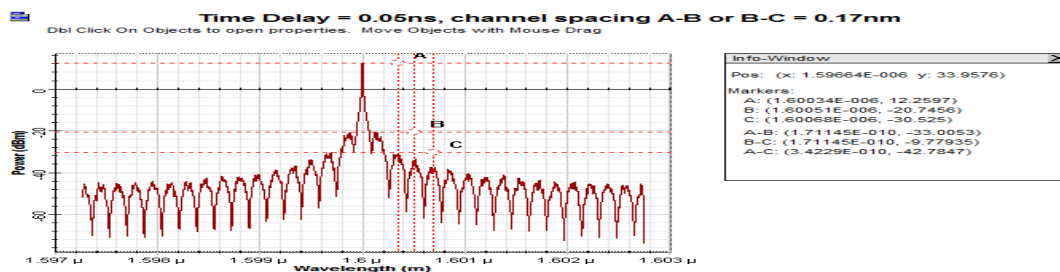


Figure B.5: Output spectra of wavelength Channel spacing and number of output channel generated at time delay of 0.05ns

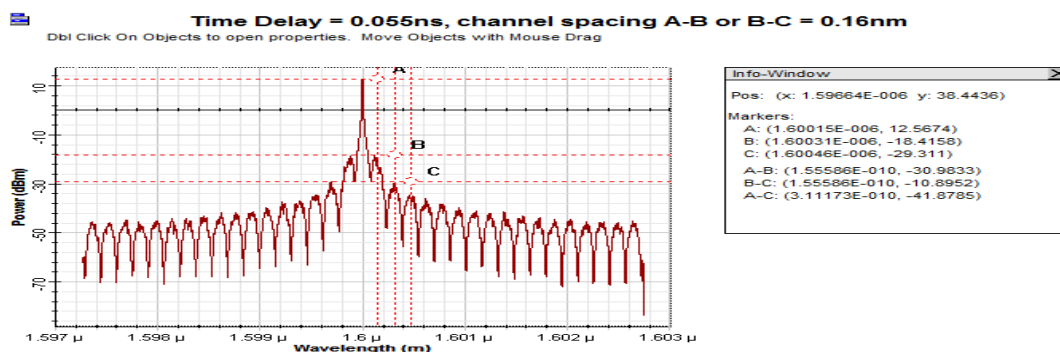


Figure B.6: Output spectra of wavelength Channel spacing and number of output channel generated at time delay of 0.055ns

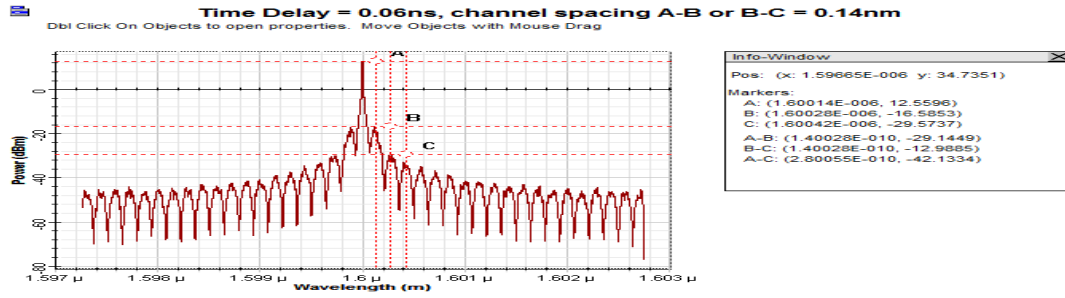


Figure B.7: Output spectra of wavelength Channel spacing and number of output channel generated at time delay of 0.06ns

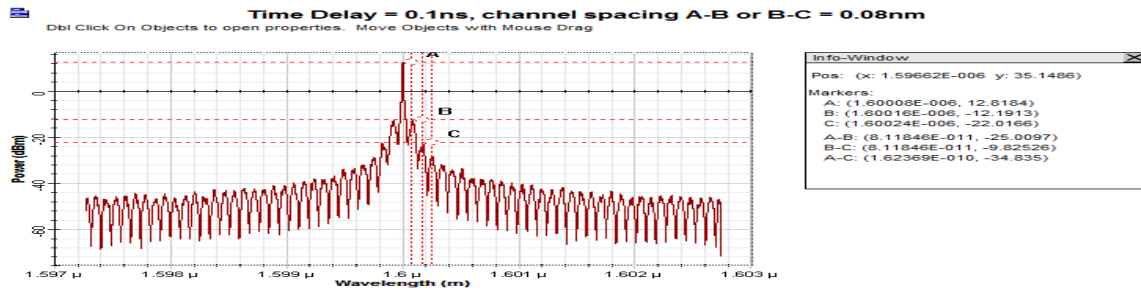


Figure B.8: Output spectra of wavelength Channel spacing and number of output channel generated at time delay of 0.1ns

Table B.1: Channel spacing and number of output channel generated at different time delay

Time delay (ns)	0.01	0.025	0.03	0.045	0.05	0.055	0.06	0.1
Channel spacing(nm)	0.8	0.33	0.29	0.18	0.17	0.16	0.14	0.08
Number of Channel	6	16	18	28	32	34	38	64

At 0.01ns of time delay, 6 channels with spacing of 0.8nm (93.7GHz) between the adjacent channels are generated as shown in figure B.1 and table B.1 while at time delay of 0.1ns, 64 channels with 0.08nm (10GHz) spacing between adjacent channels are produced as shown in figure B.8 and table B.1.

